



# Flexible self-charging power sources

Ruiyuan Liu<sup>1,2</sup>✉, Zhong Lin Wang<sup>3,4</sup>, Kenjiro Fukuda<sup>2,5</sup>✉ and Takao Someya<sup>2,5,6</sup>✉

**Abstract** | Power supply is one of the bottlenecks to realizing untethered wearable electronics, soft robotics and the internet of things. Flexible self-charging power sources integrate energy harvesters, power management electronics and energy-storage units on the same platform; they harvest energy from the ambient environment and simultaneously store the generated electricity for consumption. Thus, they enable self-powered, sustainable and maintenance-free soft electronics. However, challenges associated with materials engineering, mechanistic understanding and device design emerge when moving from individual devices to integrated systems for practical applications. In this Review, we discuss various flexible self-charging technologies as power sources, including the combination of flexible solar cells, mechanical energy harvesters, thermoelectrics, biofuel cells and hybrid devices with flexible energy-storage components. We consider exemplary applications of power-source integration in soft electronics. Finally, we provide an overview of the emerging challenges, strategies and opportunities for research and development of flexible self-charging power sources.

Efficient, lightweight and flexible power sources are notable power solutions for wireless wearable electronics, untethered soft robotics and the internet of things<sup>1–4</sup>. To meet the increasing energy demands of wearable and flexible electronics, one straightforward strategy is to increase the volumetric capacity of flexible energy-storage devices, including their energy and power densities. However, the trend of creating integrated miniaturized platforms with more and more functions presents considerable challenges for sustainable power supply<sup>5</sup>. The high power consumption of multiple components inevitably leads to early battery replacement or frequent recharging, causing inconvenience. By contrast, increasing the energy density of these flexible devices to very high levels comes with safety concerns, especially in wearable applications, which often undergo repeated mechanical stresses. Considering these factors, a flexible self-charging system that can harvest energy from the ambient environment and simultaneously charge energy-storage devices without needing an external electrical power source would be a promising solution.

A typical flexible self-charging system integrates at least two types of devices for energy harvesting and storage on a single substrate and involves three energy conversion steps. Various flexible energy-harvesting technologies can convert ambient energy into electricity. These include solar cells for harvesting light energy, triboelectrics and piezoelectrics for harvesting mechanical energy, thermoelectrics and pyroelectrics for capturing thermal energy and biofuel cells for converting biochemical energy. Light, heat, vibration, body movement or even sweat can be sources of energy in daily life.

To utilize such abundant, intermittent and randomly distributed energy sources, compatible energy-storage units that convert the harvested electricity into electrochemical energy and output electricity for consumption are indispensable for power stability and sustainability.

The total energy conversion and storage efficiency, which is the ratio of the energy output from the energy-storage device to the energy input from the ambient environment, is the most important parameter for evaluating the electrical performance of a self-charging system. This total efficiency is determined by the conversion efficiency of the energy harvesters, the storage and discharging efficiencies of the energy-storage units and the charging efficiencies between the individual components. Flexibility is another key factor, which can be achieved by using soft materials or by making the device sufficiently thin. A mechanically reliable and flexible self-charging power source should maintain normal output performance under deformations, such as bending, twisting, curling, compression or tension, to varying extents depending on the specific application. System reliability — the probability that the power source will not fail throughout a prescribed operating period — is one of the most essential considerations for real applications. This includes the reliability of the energy-harvesting and energy-storage components, power management, flexible substrate, encapsulation, electrical connection and the way these are all integrated.

Advances in materials science and device designs have increased the efficiency and reduced the thickness and weight of flexible self-charging systems since the development of the concept in the 1980s<sup>6–9</sup>.

<sup>1</sup>College of Energy, Soochow University, Suzhou, People's Republic of China.

<sup>2</sup>Center for Emergent Matter Science (CEMS), RIKEN, Saitama, Japan.

<sup>3</sup>Beijing Institute of Nanoenergy and Nanosystems, Chinese Academy of Sciences, Beijing, People's Republic of China.

<sup>4</sup>School of Materials Science and Engineering, Georgia Institute of Technology, Atlanta, GA, USA.

<sup>5</sup>Thin-Film Device Laboratory, RIKEN, Saitama, Japan.

<sup>6</sup>Department of Electrical Engineering and Information Systems, The University of Tokyo, Tokyo, Japan.

✉e-mail: ryliu@suda.edu.cn; kenjiro.fukuda@riken.jp; someya@ee.t.u-tokyo.ac.jp  
<https://doi.org/10.1038/s41578-022-00441-0>

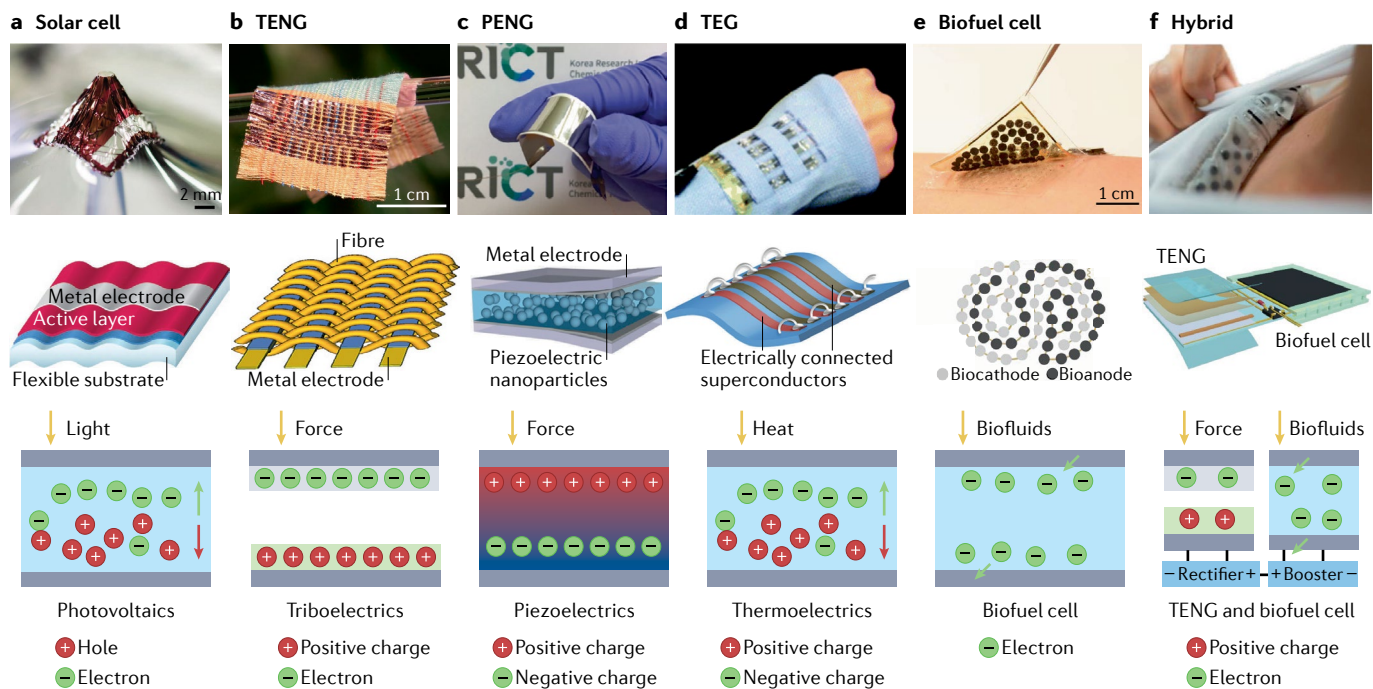


**Fig. 1 | Mechanisms of flexible ambient energy harvesters. a** | In a solar cell, light is absorbed by the active layers, generating electron–hole pairs or excitons that are subsequently separated by the built-in potential and then collected by the electrodes through the carrier-selective layers or transporting layers. **b** | In a flexible triboelectric nanogenerator (TENG), materials with stronger electron affinity will be negatively charged when they come in contact with the other materials as a result of charge transfer or electron injection from the latter. Electrons will flow back and forth through the external circuit to achieve potential equilibrium with repeated contact–separation, resulting in an alternating current. **c** | In a piezoelectric nanogenerator (PENG), the piezoelectric material is sandwiched between two electrodes connected to an external load. If a compressive or tensile force is applied, a potential difference is created, which drives the flow of electrons in the external circuit to generate currents. **d** | In a thermoelectric generator (TEG), a temperature gradient between two electrically

connected conductors or semiconductors induces diffusion of holes and electrons or ions away from the hot side, leading to a thermopotential and direct current in the external circuit. **e** | In a biofuel cell, the fuel undergoes a catalytic oxidation at the bioanode and generates electrons to reduce the oxidant at the biocathode through external circuits. **f** | In a hybrid TENG–biofuel cell device, a rectified TENG and a biofuel cell connect in parallel to harvest the mechanical and biochemical energy. All external electrical connections have been ignored. Panel **a** is adapted from REF.<sup>19</sup>, CC BY 4.0 (<https://creativecommons.org/licenses/by/4.0/>). Panel **b** is adapted from REF.<sup>10</sup>, Springer Nature Limited. Panel **c** is adapted with permission from REF.<sup>174</sup>, Royal Society of Chemistry. Panel **d** is adapted with permission from REF.<sup>42</sup>, Royal Society of Chemistry. Panel **e** is adapted with permission from REF.<sup>14</sup>, AAAS. Panel **f** is adapted from REF.<sup>130</sup>, CC BY 4.0 (<https://creativecommons.org/licenses/by/4.0/>), and REF.<sup>175</sup>, CC BY 4.0 (<https://creativecommons.org/licenses/by/4.0/>).

The efficiency of integrated devices has steadily risen with progress in the technology of individual components and optimized integration. Superior flexibility or stretchability can be realized by using advanced device configurations with fibre shapes or wrinkled structures, or by reducing the device thickness<sup>10,11</sup>. Innovations in materials engineering and manufacturing technology have enabled the fabrication of ultrathin devices with thicknesses down to the micrometre scale while exhibiting high power or energy density. Wearable sensors and soft robotics have been operated successfully with the energy harvested from body motion<sup>9,12</sup>, sweat<sup>13,14</sup> or sunlight<sup>15</sup>, demonstrating the potential of flexible self-charging power sources.

In this Review, we highlight the integration of flexible solar cells, mechanical energy harvesters, thermoelectrics, biofuel cells and hybrid devices with flexible energy-storage components on a single platform. We discuss power management strategies for effective energy transfer between energy harvesters and energy-storage units. We then survey the applications of these self-charging power sources in soft electronics. Finally,

we outline the scientific challenges related to improving performance and present strategies in materials engineering and device designs to address them.

### Flexible energy harvesters

Energy harvesters convert ambient energy — such as light, mechanical energy, heat and biochemical energy — into electricity (FIG. 1 and TABLE 1).

#### Photovoltaic solar cells

Solar cells convert light energy into electricity through photovoltaic effects (FIG. 1a). A typical solar cell contains active layers, carrier-selective layers and electrodes. Light is absorbed by the active layers, generating electron–hole pairs, or excitons, which are subsequently separated by the built-in potential and then collected by the electrodes through carrier-selective layers or transporting layers. Because the total thickness of the active layers in a device ranges from a few hundred nanometres to a few micrometres, reducing the thickness of the flexible substrate can increase device flexibility and power density and lower weight<sup>16–19</sup>. To date, the power conversion

efficiencies (PCEs) of single-junction flexible perovskite solar cells and flexible organic solar cells under AM 1.5 G standard conditions (Air Mass 1.5 Global standard, representing terrestrial solar spectral irradiance on a surface of specified orientation under one and only one set of specified atmospheric conditions with light intensity of  $100 \text{ mW cm}^{-2}$ ) have reached 21.73% and 16.61%, respectively<sup>20,21</sup>. For weak light conditions, the PCE of flexible perovskite solar cells has increased to 23.33% at 400 lx and 28.63% at 5,000 lx from a white light-emitting diode<sup>22</sup>. A flexible organic solar cell with a PCE of 20.5% under indoor light illumination of 1,500 lx has also been reported<sup>23</sup>.

#### Triboelectric nanogenerators

Triboelectric nanogenerators (TENGs) harvest mechanical energy based on the triboelectric effect, which is the coupling of contact electrification and electrostatic induction (FIG. 1b). Contact separation between two materials causes charge transfer between the surfaces, and the charges or electrons flow through external circuits to maintain electrostatic equilibrium; thus, the device generates an alternating electrical output<sup>24</sup>. A flexible TENG can be fabricated from soft materials,

such as polymers, metals, paper, semiconductors or hydrogels. The peak power density of flexible TENGs has increased from a few microwatts to  $50 \text{ mW cm}^{-2}$  since 2012, and they also have excellent flexibility, outstanding stretchability and multifunctionality<sup>25–30</sup>.

#### Piezoelectric nanogenerators

The piezoelectric effect is the ability of certain materials — piezoelectrical materials — to generate an electric charge in response to applied mechanical stress. Piezoelectric nanogenerators (PENGs) work based on the direct piezoelectric effect and a change in the electrical polarization induced by breaking central symmetry of the crystal structure in non-centrosymmetric piezoelectric materials. The stress-dependent change in polarization generates an internal potential difference across the material, which acts as the driving force for the flow of electric charges in external circuits to generate an alternating current (AC) (FIG. 1c). The polarized charge density is determined by the piezoelectric coefficient of the materials and the applied stress. The first PENG was fabricated in 2006 using aligned zinc oxide (ZnO) nanowires and the peak power density of flexible devices has improved in that time from  $\sim 0.5 \text{ pW}$  per nanowire to a few milliwatts per device<sup>31–36</sup>.

Table 1 | Comparison of flexible energy harvesters and energy-storage units

Category	Device	Energy source	Mechanism	Active materials	Outputs	Characteristics	
						Positives	Negatives
Energy harvesters	Solar cell	Light: the Sun, indoor/outdoor light	Photovoltaic effect	Semiconductors	DC A few tens of $\text{mW cm}^{-2}$ A few tens of $\text{W g}^{-1}$ (at a light intensity of $100 \text{ mW cm}^{-2}$ ) $\sim 1 \text{ V}$	High power output Lightweight Ultrathin design	Unstable
	TENG	Mechanical energy: wind, wave, body motion	Triboelectrification and electrostatic induction	Diverse	AC $\mu\text{W}$ to $\text{mW cm}^{-2}$ (peak) $\mu\text{W}$ to $\text{mW g}^{-1}$ (peak) Up to kV (peak)	Ubiquitous Multiple designs Robust	Low energy
	PENG						
	TEG	Heat: the Sun, body, device	Thermoelectric/Seebeck effect	Thermoelectrics	DC $\sim \mu\text{W cm}^{-2}$ $\sim \text{mV K}^{-1}$	Commercially available	Low energy Thermal matching
	Biofuel cell	Electrochemical energy: body fluid	Electrochemical reaction	Biofuels, catalysts	DC A few $\text{mW cm}^{-2}$ $\sim 1 \text{ V}$	On-body available	Low power and energy
Energy-storage devices	Supercapacitor	Chemical energy: electricity or chemicals	Electric double-layer capacitance or pseudocapacitance	Carbon materials, organic materials, metal compounds, Si	DC Up to $10,000 \text{ mW g}^{-1}$ 1–4 V	High power Long cycle life	Low energy density
	Battery		Electrochemical redox reactions				

AC, alternating current; DC, direct current; PENG, piezoelectric nanogenerator; TEG, thermoelectric generator; TENG, triboelectric nanogenerator.

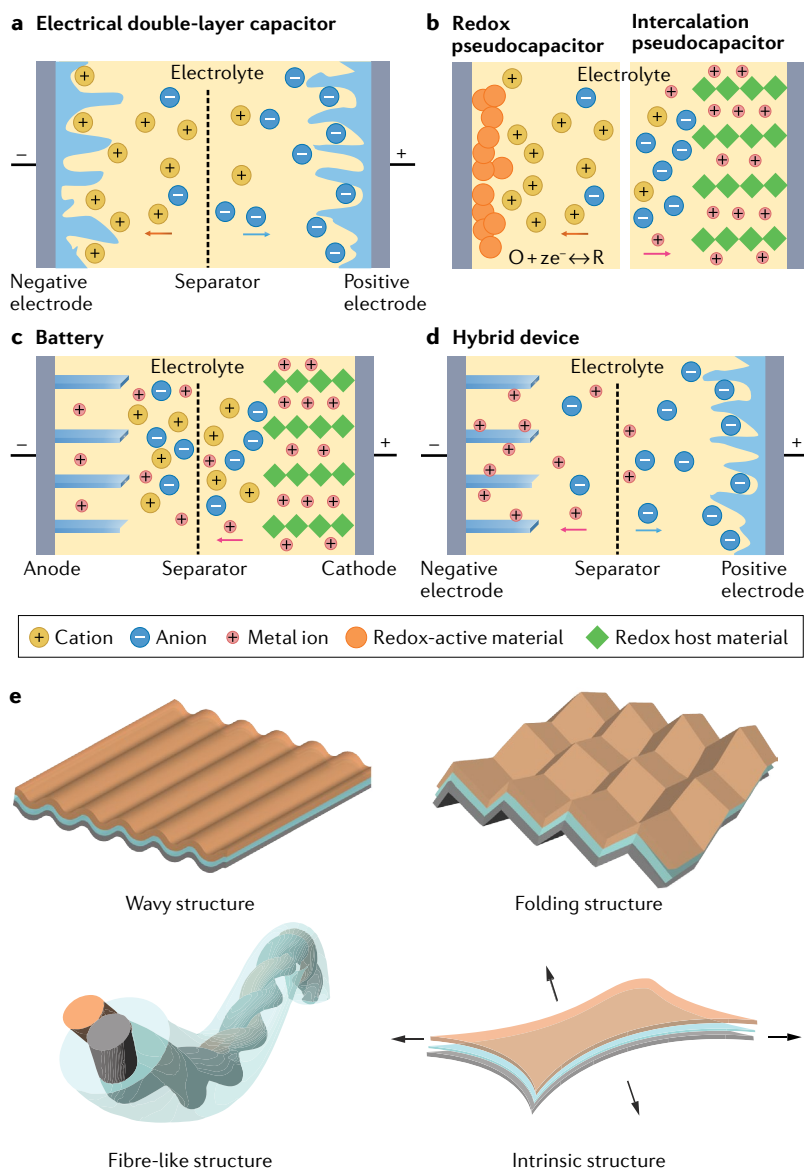


**Fig. 2 | Charging mechanisms of flexible energy-storage devices.** Supercapacitors store the charge through the reversible electrostatic adsorption of electrolyte ions, such as an electrical double-layer capacitor (panel **a**), or through faradic surface redox reactions or intercalations (panel **b**), which is a pseudocapacitor. A lithium-ion battery stores electrical energy through reversible insertion and extraction of lithium ions from the electrode materials, undergoing electrochemical redox reactions in the bulk (panel **c**). Hybrid energy-storage devices combine capacitive materials and battery-type materials and can balance high energy density and high power density in a single cell (panel **d**). Strategies for flexible or stretchable energy-storage devices (panel **e**). A wavy device uses conventional materials to construct a buckled pattern that accommodates flexure or stretching by decreasing the amplitude of the waves. A folding structure accommodates deformation by folding of planar devices, similar to a wavy structure. Fibre-like energy-storage devices can be achieved using coaxial or twisted fibres to enable flexibility and stretchability. An intrinsically stretchable device differs from the other types by using individual stretchable components, which offers the greatest manufacturing compatibility. Panel **e** is reprinted with permission from REF.<sup>65</sup>, Wiley.

### Thermoelectric generators

Thermoelectric generators (TEGs) convert heat energy into electrical energy through the Seebeck or the Soret effect (FIG. 1d). A temperature gradient between two electrically connected conductors or semiconductors induces the diffusion of carriers or ions away from

the hot side, leading to the development of a thermo-potential and direct current (DC) in the external circuit. The figure of merit  $ZT$  is the key parameter for assessing the desirability of thermoelectric materials. Most state-of-the-art thermoelectric materials exhibit maximum  $ZT$  values of 2–3 and the power densities of the flexible devices have reached several tens of microwatts per square centimetre<sup>37–42</sup>, enabling their application in wearable electronics<sup>43–45</sup>.

### Biofuel cells

Biofuel cells rely on redox reactions of various biofluids to convert biochemical energy into electricity (FIG. 1e). They are based on oxidizing biocatalysts, which promote the oxidation reaction of fuels at the bioanode, and reducing biocatalysts, which promote the reduction to water at the biocathode; the flow of electrons at the external electric circuit generates current and power. The output current depends mainly on the concentration of the chemical fuel in the biofluids and the efficiency of electron transfer between the biocatalyst and the electrode. The power density has improved to 3.5 mW cm<sup>-2</sup> since the first milliwatt-level flexible sweat biofuel cell was developed<sup>14,46–48</sup>.

### Hybrid energy harvesters

Because various forms of ambient energy are available as energy sources in the working environment — especially for mobile electronic devices — an effective strategy to enhance the power density and sustainability is to use hybrid energy harvesters. These integrate different devices on the same platform to simultaneously harvest one or more kinds of energy, compensating for the intermittent nature of a single energy source. The first hybrid device, reported in 2009, combined a solar cell and a PENG to harvest solar and ultrasonic energy<sup>49</sup>. Other hybrid harvesters include integrated TENGs and biofuel cells (FIG. 1f), TENGs and solar cells, TENGs and PENGs, and TENGs and TEGs<sup>10,50,51</sup>.

### Flexible energy-storage devices

Energy-storage devices store charge through several mechanisms (FIG. 2).

#### Supercapacitors

Supercapacitors, or electrochemical capacitors, store charge through the reversible electrostatic adsorption of electrolyte ions or faradic surface redox reactions. A flexible supercapacitor consists of two electrodes with current collectors, an electrolyte and a separator. Electrical double-layer capacitors work through reversible electrostatic ion adsorption at the surface or porous structure of high-surface-area carbon materials without any chemical reaction (FIG. 2a). Pseudocapacitors store energy through surface redox reactions at transition-metal oxide, carbide, nitride or conducting polymer electrodes<sup>52–54</sup> (FIG. 2b).

#### Rechargeable batteries

Rechargeable batteries, or secondary batteries, store energy through reversible electrochemical redox reactions in electrodes under an applied voltage and

current (FIG. 2c). As chemical reactions occur in the bulk of the electrode materials, batteries can deliver very high energy densities (up to  $\sim 300 \text{ Wh kg}^{-1}$ ). Enlarging the chemical potential difference between the anode and the cathode, using nanomaterials and engaging a stable electrolyte with high-voltage tolerance are effective strategies to increase the energy-storage ability of a battery<sup>55–58</sup>.

#### Hybrid energy-storage devices

Hybrid energy-storage devices combine different charge-storage mechanisms in a single cell (FIG. 2d). Supercapacitors have high power density and low energy density, whereas batteries usually exhibit high energy density and low power density<sup>59</sup>. Hybrid devices, which take advantage of both battery-type materials and capacitive materials, aim to simultaneously produce high energy density and high power density, striking a balance between both<sup>60–64</sup>.

Developing flexible or even stretchable energy-storage devices is particularly important for wearable devices (FIG. 2e). Among these, batteries currently have the most promise to constantly power wearable electronics; improving their flexibility, energy density and safety are key to an efficient and reliable self-charging power source<sup>65</sup>.

#### Flexible self-charging systems

Self-charging systems harvest distributed forms of energy that are available from the human body and the surrounding environment, and simultaneously store the electricity for consumption (FIG. 3 and TABLE 2).

#### Photo-charging systems

Systems that charge with light can be designed with two, three or four electrodes (FIG. 3a). The first two-electrode photo-charging battery, which incorporated a dye-sensitized photoactive layer on a charge-storage layer, was reported in 2002 (REF.<sup>66</sup>). This was followed in 2004 by a two-electrode photo-charging capacitor that integrated a dye-sensitized photoactive layer with two layers of active carbon particles<sup>67</sup>. These pioneering works inspired the combination of direct solar energy harvesting and storage in one unit. However, because of the complex interactions involving photo-assisted redox reactions at the photo-electrode and electrochemical reactions at the electrode of energy-storage units in liquid electrolyte, the system performance of two-electrode designs is still poor. A three-electrode photo-charging system comprises an individual solar cell and an energy-storage unit with a common electrode, which prevents direct contact between the photoactive layer and the electrolyte; it thus exhibits a better interface stability than that of a two-electrode system<sup>7</sup>. The common electrode collects the generated photocarriers to store electricity. Four-electrode systems connect the solar cells and energy-storage parts externally, offering the flexibility of adjusting the outputs of the solar cells according to the input requirements of the energy-storage parts.

The total efficiency of a photo-charging system — the ratio of energy output from the energy-storage devices to energy input from light — is key to evaluating its

performance. The PCE of solar cells is the theoretical maximum for the total efficiency, neglecting the inevitable energy loss during energy transfer. To achieve a high total efficiency, the properties of the common electrode and certain matching principles are critical, as is the optimization of individual devices.

The common electrode must be electrically conductive, mechanically flexible and electrochemically stable, and metal, carbon materials, metal oxides and conductive polymers have been widely employed<sup>11,68–70</sup>. By applying a polymeric active electrode of the supercapacitor onto the rear metal electrode of an ultrathin flexible organic solar cell, which serves as a common electrode that facilitates direct energy storage and avoids external wire connections, a 50- $\mu\text{m}$ -thick device with a total efficiency of 6% could be achieved<sup>70</sup>. Sometimes, metal common electrodes also act as flexible substrates, especially in fibre-based devices, including coaxial and twisted structures. For 1D photo-charging wearable devices, carbon fibres are the best candidates because of their high stiffness, intrinsic flexibility and light weight. One challenge in using carbon materials in common electrodes is their low electrochemical activity, which can be overcome by combining them with metal oxides or conducting polymers in compound electrodes<sup>53,69</sup>.

Proper matching of parameters, including voltages, currents and capacitances, between solar cells and energy-storage devices is important for all photo-charging systems and this can be addressed by power management circuits and a rational device design. The device design includes electrical connections and internal material configurations. Most single-junction solar cells generate output voltages below 1 V, which is sufficient to charge some supercapacitors, but not enough for batteries. In principle, the voltage of the solar cells at the maximum power point (MPP) should be matched as closely as possible to the maximum charging voltage of batteries. Based on this, high total efficiencies of over 14% and 20.1% have been achieved with the integration of rigid III–V and perovskite/silicon tandem solar cells, respectively, with redox flow batteries using high-voltage redox couples in neutral solvent<sup>71,72</sup>. A mismatch in the photocurrent could lead to energy loss and device deterioration; thus, proper device design is necessary to either fully charge the energy-storage units or utilize the excess current<sup>73</sup>. A clear capacitance matching effect has been observed as well<sup>70</sup>. Overall, maximizing the power output of solar cells while minimizing energy loss due to parameter mismatch is especially critical for monolithic integrated photo-charging devices.

The total efficiency of integrated devices has continuously improved with the development of various solar cells. Flexible perovskite solar cells show PCEs greater than 20%, outperforming their counterparts, which has led to the most efficient photo-charging systems so far<sup>74,75</sup>. However, their lead-based compositions pose a poisonous problem and should be addressed by either robust encapsulation or alternative compositions<sup>76,77</sup>. The incorporation of non-fullerene acceptors has improved the performance of flexible organic solar cells and PCEs have exceeded 16.5%<sup>78,79</sup>. When solar cells are rationally matched with flexible supercapacitors and

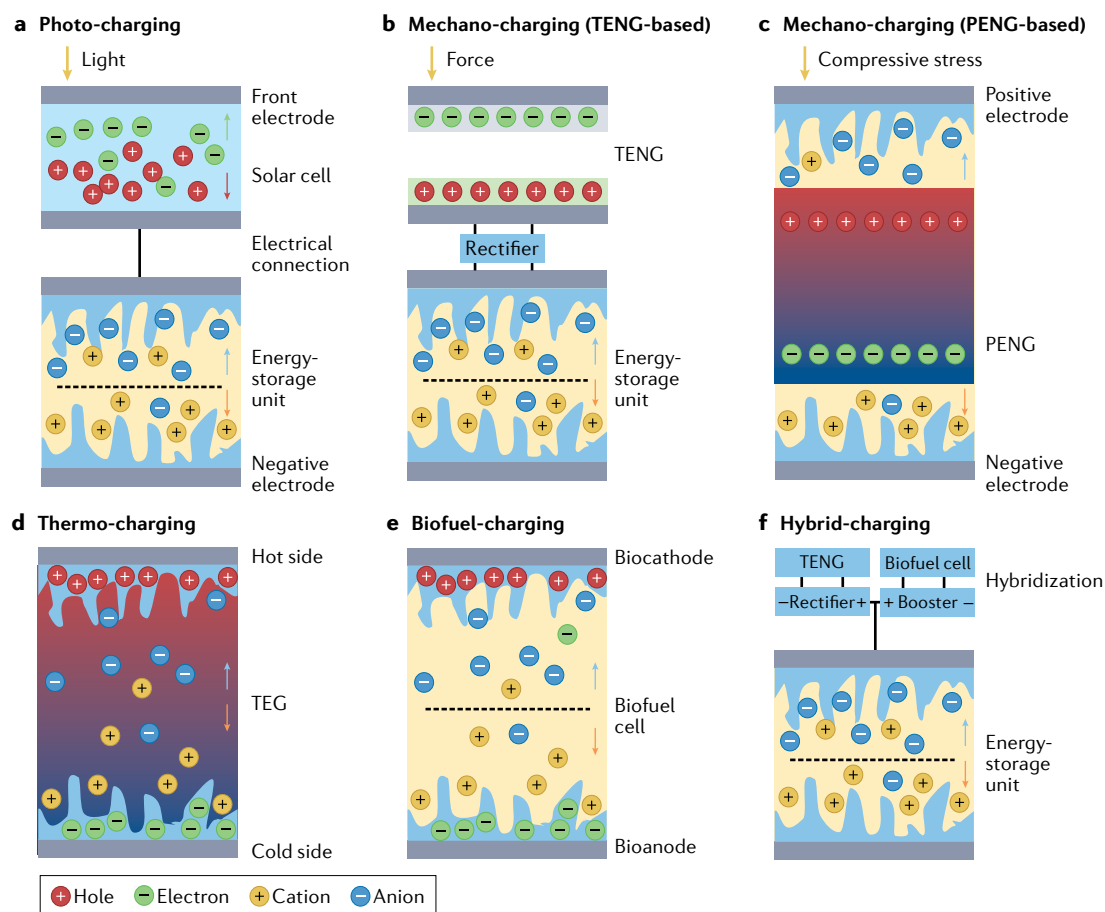


**Fig. 3 | Mechanisms of self-charging power sources.** **a** | A photo-charging system comprises an individual solar cell and an energy-storage unit with electrical connections. The solar cell converts light energy into electricity and performs charging through a photo-electrode (two-electrode system), a common electrode (three-electrode system) or external connections (four-electrode system). **b** | A four-electrode triboelectric nanogenerator (TENG)-based self-charging system connected by a rectifier. The electrical outputs of most TENGs are in pulsing and alternating forms, requiring rectifiers to convert the alternating current to direct current before charging. **c** | A two-electrode piezoelectric nanogenerator (PENG)-based self-charging system using a piezoelectric field induces electrochemical redox reactions or ion migration in the electrodes of batteries or supercapacitors. A self-charging cycle is triggered by a compressive force that increases the potentials of the two electrodes until the system reaches a new chemical equilibrium. **d** | A two-electrode thermo-charging device sandwiches the thermoelectric electrolyte or conductor between the electrodes of the energy-storage unit. The self-charging is driven by a thermovoltage, induced by a temperature difference applied to the electrode–electrolyte–electrode stack, through thermally driven ion movement or the thermogalvanic effect of the redox couples. **e** | A two-electrode biofuel-charging device has the same electrodes, where electrons directly transfer with the redox enzymes to perform energy harvesting and storage. **f** | A hybrid-charging system comprises a biofuel cell and a rectified TENG as energy harvesters and a supercapacitor as an energy-storage unit. The device harvests biomechanical and biochemical energy from human activities simultaneously. In addition to possessing higher charging speed than one harvester alone, the two harvesters exhibit complementary effects, including ‘fast boosting’ and ‘extended harvesting’. TEG, thermoelectric generator.

batteries, the photo-charging system possesses the most efficient self-charging power sources.

#### Mechano-charging systems

**TENG-based systems.** The electrical outputs of most triboelectric devices are in pulsing and alternating forms, requiring rectifiers to convert them to DC before driving electronics or charging. In addition, TENGs function through the coupling of contact electrification and electrostatic induction between two surfaces, the induced surface charges of which are neutralized upon exposure to moisture or liquids. Direct integration using

a common electrode or sandwiching the energy harvesters inside energy-storage devices is, therefore, not possible. Instead, a four-electrode configuration connected by a rectifier on the same flexible platform is a feasible design (FIG. 3b). Because TENGs are capacitive energy-harvesting technologies that generate high voltages (up to kV) and low currents (usually in nA or  $\mu$ A), specific integrated matching parameters including impedance, capacitance and voltage are crucial for efficient self-charging, which relies on power management<sup>80–82</sup>.

Fibres, yarns and textiles are ideal flexible forms for wearable devices. Conductive supporting fabrics can be

prepared using metal or carbon wires<sup>83</sup> and by depositing conductive elements onto polymer yarns<sup>84,85</sup>. The fabrics generate electricity by friction, body motion and hand touching at very low frequencies<sup>10,12,84,85</sup>. A power textile, crafted from fabric TENGs and woven supercapacitors by a traditional weaving method, was able to self-charge at a rate of  $1.4 \mu\text{C s}^{-1}$  at 1.5 Hz of arm swaying<sup>86</sup>. Waterproof and elastic triboelectric materials, such as silicone and polydimethylsiloxane, have enabled washable and stretchable textiles<sup>87</sup>. Direct printing or dyeing of active materials onto fabrics is another facile technology<sup>88</sup>.

Thin-film and bulk flexible self-charging systems can be constructed by stacking the devices or assembling them in parallel. Vertically stacked devices are more compact and have potentially higher areal power densities than parallel-design devices at comparable performance values<sup>89,90</sup>. In addition to integrating one TENG with one energy-storage unit, the latter can also be sandwiched between two TENGs, doubling the charging input from one trigger<sup>91</sup>. Most designs aim at harvesting low-frequency compressive mechanical energy and suffer from insufficient charge, but a high-frequency vibrating and implantable TENG can harvest ultrasound

energy and charge a lithium-ion battery at a rate of  $166 \mu\text{C s}^{-1}$  in water, more than 100 times faster than TENGs in previous reports<sup>29</sup>.

Although TENGs are promising, their low performance is still a bottleneck for efficient self-charging. While the material choices are diverse, certain principles can be followed to maximize the power output. The difference in the electron affinities of the materials for contact electrification should be as large as possible to achieve a high charge density, which can be realized by material selection or chemical functionalization. Nanostructures can be effective for enlarging the contact area. It is worth noting that some highly efficient designs with optimized individual materials and devices have not been reported in integrated systems<sup>26,92</sup>. Furthermore, the use of conventional rigid rectifiers has hampered the development of all-flexible self-charging systems, limiting the monolithic design and decreasing system efficiency. Developing thin and flexible rectifiers based on thin-film semiconductors is a possible solution. The other strategy is to eliminate the rectifier by employing a direct-current TENG, which converts mechanical energy into direct-current electricity based on charge accumulation, tunnelling effects or dielectric breakdown<sup>93–96</sup>. This emerging technology can enable direct charging or powering, although further efforts are required to understand the detailed working mechanism.

**PENG-based systems.** The stress-induced potential of PENGs facilitates their unique self-charging ability by adapting piezoelectric materials as separators or solid-state electrolytes between the electrodes of the energy-storage devices<sup>9</sup>. A piezoelectric field is created in the piezoelectric materials with compressive force, resulting in electrochemical redox reactions or ion migration — a piezoelectrochemical conversion process (FIG. 3c). The potentials of the two electrodes increase until the system reaches a new chemical equilibrium during self-charging. Once the applied compressive force is withdrawn, the piezoelectric potential disappears and another new chemical equilibrium is built. Repeatedly applying and releasing forces can accumulate cyclic charge storage by converting mechanical energy into chemical energy.

Using porous piezoelectric materials as both nanogenerators and separators is key to high device performance, characterized by the simultaneous demonstration of ideal piezoelectric properties, electrochemical stability and ionic conductivity. To combine these functionalities, piezoelectric polyvinylidene fluoride (PVDF) and its composites have been the most widely used workarounds in PENG-based self-charging devices<sup>9,97</sup>. A polarized PVDF film was used as a separator in a battery to drive the migration of Li ions along the piezopotential to conduct self-charging<sup>9</sup>. Porous PVDF membranes were subsequently developed to induce more confined strain in the axial direction by the nanopores<sup>98,99</sup>. Immobilized mesoporous and composite films serving as both piezoelectrolytes and piezoseparators enable all-solid-state flexible devices with improved charging efficiency<sup>100</sup>. The integration

Table 2 | Available energy around a human<sup>14,23,171–173</sup>

Energy source	Power	Notes
Breath at exhalation	1 W	A 68-kg person with an air intake rate of approximately 30 litres per minute
Finger motion	6.9 mW	Assuming a moderately skilled user typing at 40 words per minute, considering multiple keystroke combinations
	19 mW	A fast QWERTY typing (90 words per minute) at 7.5 keys per second
Blood pressure	0.93 W	Assuming an average blood pressure of 100 mm of Hg, a resting heart rate of 60 beats per minute and a heart stroke volume of 70 ml passing through the aorta per beat
Arm motion	60 W	For a particular 58.7-kg man with arm mass of 3.2 kg. The distance through which the centre of mass of the lower arm moves for a full bicep curl is 0.335 m. Empirically, bicep curls can be performed at a maximum rate of 2 curls per second and lifting the arms above the head can be performed at 1.3 lifts per second. The maximum power generated by arm lifts is 60 W
	3 W	Violin playing and housekeeping
Walking	67 W	A 68-kg man using the fall of the heel through 5 cm, at two steps per second
Body heat	2.4–4.8 W	Assuming that all of the heat radiated by the body while sitting is captured and perfectly transformed into power, between normal body temperature (36.5–37.5 °C) and room temperature (20–27 °C)
Sweat	$3.5 \text{ mW cm}^{-2}$	From the recorded power densities of wearable biofuel cells
Light	$16.61 \text{ mW cm}^{-2}$	Calculated from the recorded power conversion efficiencies of single-junction flexible organic solar cells under AM 1.5 G standard conditions (light intensity of $100 \text{ mW cm}^{-2}$ )
	$97 \mu\text{W cm}^{-2}$	Calculated from the recorded power conversion efficiencies of single-junction flexible organic solar cells under indoor light illumination of 1,500 lx

with supercapacitors is similar to that with batteries, mainly based on 2D electrode materials<sup>101,102</sup>.

PENG-based devices can easily self-charge under various repeated deforming conditions, maintaining almost the same architectures of batteries or supercapacitors. However, most current reports focus on demonstrating prototypes of self-charging ability using different materials and designs, rather than improving and quantifying the output performance. The peak output voltage of PENGs has rapidly increased from a few millivolts to hundreds of volts in the past few years, which is sufficiently high for self-charging<sup>31,36</sup>. However, the output current at the nA to  $\mu$ A level is still too small for efficient device charging because of the limited surface polarization charges. The lack of a clear figure of merit for performance makes it difficult to directly compare different devices, hampering further development. In particular, other than the proposed piezoelectrochemical conversion theory<sup>103</sup>, little is known about their self-charging mechanism because of the complexity of interactions between the piezoelectrical potentials and the electrochemical potentials of the energy-storage units. The influence of the piezoelectrical potential on ion migration — which should be substantial because most of the ions are transported through the piezoseparator where the piezoelectrical potential is located — is also not well investigated. The long-term effects of direct mechanical stress on energy-storage devices remain a concern.

#### Thermo-charging systems

Depending on whether they contain redox couples, most monolithic devices that charge with heat fall into two categories: redox-free ionic thermoelectric supercapacitors based on the thermo-diffusion of ions in electrolytes caused by the Soret effect, and thermal–electrochemical cells based on temperature-dependent electrochemical redox potentials caused by the thermogalvanic effect.

**Ionic thermoelectric supercapacitors.** An ionic thermoelectric supercapacitor consists of an ionic thermoelectric electrolyte or conductor sandwiched between the electrodes of the supercapacitor (FIG. 3d). The temperature difference applied to the electrode–electrolyte–electrode stack induces a thermovoltage through thermally driven ion movement, which charges the supercapacitor. Once the temperature difference and external connection are removed, the charging process is terminated and the ions diffuse back with the charges stored at the electrode–electrolyte interface, resulting in a voltage that is opposite to the original thermovoltage.

The device performance can be increased through materials engineering. The interaction between the ions and electrolyte can be tailored by mixed ionic–electronic composites to increase the potential differences; typical ionic thermoelectric materials include water-based polyelectrolytes, ionic liquid polymer gels and their hybridization. Alternatively, preparing the electrode with a high surface area and electrical conductivity improves the storage efficiency and stability. An ammonia-treated polymeric electrolyte exhibited a high ionic Seebeck coefficient of  $11.1 \text{ mV K}^{-1}$ , leading to 2,500 times higher stored energy in the integrated device than by externally

connected charging<sup>104,105</sup>. An improved design uses polystyrene sulfonic acid as both a solid electrolyte and a voltage generator, which can maintain a charged state for more than 24h without obvious self-discharging<sup>91</sup>. Further investigation of ion–ion interactions and the interaction between ions and the dipole moment has pushed the Seebeck coefficient to over  $24 \text{ mV K}^{-1}$  (REFS<sup>106,107</sup>).

**Thermal–electrochemical cells.** In a thermal–electrochemical cell, two electrodes in contact with an electrolyte containing a redox couple are kept at different temperatures. Thermovoltage is generated by the thermogalvanic effect of the redox couples. An external electrical connection leads to oxidation on the anode and reduction on the cathode, and electrical charging occurs as electrons move from the anode to the cathode through an external circuit.

The maximum thermovoltage that can be generated in a thermal–electrochemical cell is determined by the Seebeck coefficient of the redox couple, as a result of entropy change during oxidation or reduction<sup>108</sup>. In terms of materials, choosing appropriate redox couples and increasing the entropy change, affected by structural changes in the redox species, are effective ways to obtain a higher potential difference. Ferricyanide/ferrocyanide, iodide/triiodide and copper-based redox couples are the most well-studied practical redox couples, given their electrochemical reversibility, operational stability and material availability<sup>108,109</sup>. Strong chaotropic cations (guanidinium) and highly soluble amide derivatives (urea) have been introduced into aqueous ferricyanide/ferrocyanide to enlarge the entropy difference of the redox couple and improve the Seebeck coefficient from  $1.4$  to  $4.2 \text{ mV K}^{-1}$  (REF<sup>110</sup>). Electrodes with a high surface area and conductivity and electrolytes with good mass transport properties are necessary to achieve an adequate current density. Asymmetric electrodes can generate a synergistic voltage through the thermogalvanic effect of the redox couple and a temperature-induced pseudocapacitive effect of the graphene oxide electrode, leading to a coefficient of  $5 \text{ mV K}^{-1}$  and heat-to-electricity conversion efficiency of  $2.8\%$ <sup>111</sup>.

#### Biofuel-charging systems

Wearable biofuel cells are among the most attractive on-body energy-harvesting devices, especially for skin electronics, which generate electric energy directly from reactions with biofluids, such as tears, blood, interstitial fluid and sweat<sup>112</sup>. However, wearable biofuel cells and, thus, biofuel-charging systems are still in the very early stages of development<sup>112–114</sup>. The limitations of body fluids for voltage output are that they require effective energy storage for a sustainable power supply. Distinctively, biofuel cells and energy-storage units can share the same electrodes, where electrons directly transfer with the redox enzymes to perform energy harvesting and storage (FIG. 3e). This concept has been demonstrated using engineered electrodes, redox mediators and printing technologies.

The first biofuel-charging device integrated a glucose/oxygen biofuel cell and a supercapacitor, using

a carbon nanotube (CNT) matrix as a shared electrode<sup>115</sup>. The compressed CNT matrix/enzyme design favours direct electron transport with the enzymes, where the bioanode undergoes oxidation of glucose to gluconolactone, transferring electrons to the CNT matrix. At the biocathode, for the reduction of oxygen to water, electrons are received from the matrix through the external circuit. The supercapacitor is recharged from the continuous energy conversion of the biocatalysts of glucose and oxygen. This compact configuration led to high operational stability, with a constant discharge pulse of 2 mW for more than 4,000 cycles over five days.

A single-polymer-based Nernstian biosupercapacitor was developed using a redox hydrogel for both the bioanode and the biocathode to realize self-charging<sup>116</sup>. The self-charging operation of the cell is based on the activity gradient of polymer-bound Os complexes, driven by enzymatically catalysed glucose oxidation and reduction of oxygen. The selection and design of such polymers should follow certain principles: a redox potential between the prosthetic groups of the electrode enzymes that can guarantee a high driving force for the electron transfer between the enzymes and the redox mediator, sufficient mass of materials to ensure a high pseudocapacitance and a low affinity towards molecular oxygen to avoid parasitic oxygen reduction at the bioanode. A voltage of 0.45 V was achieved with a low leakage current.

In an example that extended such integration to stretchable devices, a sweat-based biofuel cell and a MnO<sub>2</sub>/CNT-based supercapacitor were printed on the two sides of a textile<sup>117</sup>. Both devices were screen-printed with optimal elastomer-containing ink formulations and serpentine structure patterns that could maintain stable electrochemical performance under mechanical deformation. This design allowed a stabilized electrical output density of 252  $\mu\text{W cm}^{-2}$  from a single biofuel cell mounted to a human subject arm, which was able to charge the supercapacitor to 0.4 V.

The development of integrated biofuel-charging devices is far behind that of other device types. As wearable biofuel cells rely on the availability of chemical fuel in biofluids, device stability has always been the most crucial challenge. For example, most proof-of-concept wearable biofuel cells still depend on exercise for sweat generation, which greatly limits their further application<sup>118</sup>. The efficiency of the cells is strongly influenced by body conditions and the active surface, or the direct contact area with the skin or tissue, requiring more physical interface conformability for integrated devices than others. Increasing the loading of active electrode materials such as enzymes and mediators on flexible substrates is an effective strategy to increase the power density.

### Hybrid-charging systems

The intermittent presence of extractable energy from the working environment is one of the greatest challenges for a sustainable and stable power supply. Combining different types of energy harvesters in one system can vastly improve the overall charging efficiency, especially when the energy source is weak or unavailable. This can be extremely important, because in the internet of things

or in soft electronics in the era of 5G, every small part of energy counts towards system operation. To date, most flexible hybrid systems have included mechanical energy harvesters because of the diversity of mechanical energy sources and the facile integration of TENGs or PENGs with other devices (FIG. 3f).

**Mechanical and light energy.** For hybrid-charging systems based on TENGs and solar cells, fibre-shaped devices that simultaneously harvest light energy and mechanical energy are the most favourable<sup>119–122</sup>. The devices can be hybridized in parallel on a single fibre or woven together onto a textile. Ideally, the flexible TENG component harvests energy from wind, vibration or body motion and the solar cell maintains a certain degree of mechanical durability for possible deformation or friction. An exceptional example is a polymer-fibre-based hybrid textile fabricated using a shuttle-fly process that can charge a 2-mF commercial capacitor to 2 V in 1 min under ambient sunlight with car movement or blowing wind<sup>10</sup>. However, in all the reported self-charging systems, the efficiency of the solar cell component is relatively low — less than half the value of the corresponding stand-alone device<sup>78,123</sup>. A reasonable hybrid system should retain a comparable performance from each energy harvester and then consider device designs and power management.

**Mechanical and thermal energy.** Mechanical movements, such as friction or rotation, usually generate waste heat that increases the system temperature and decreases efficiency. In this regard, hybrid systems of TENGs or PENGs with thermoelectrics or pyroelectrics not only harvest two kinds of energies in one device but the device designs also improve the cost-effectiveness of the system<sup>50,124–127</sup>. These types of hybrid pairs usually adopt vertically stacked designs to directly harvest mechanical energy and thermal energy from a single trigger, such as friction of textiles or touch with a human finger. Optimization strategies, such as tuning the operating frequency and feature size, have been designed to maximize the hybrid interface area and prevent thermal saturation<sup>50</sup>. In contrast to simple hybrid devices that merely improve charging performance over a single component, optimized devices feature a higher electrical output than would be expected from the addition of constituent parts — a synergistic effect in output performance.

**Mechanical and biochemical energy.** Hybrids of TENGs and biofuel cells are distinct in that their complementary functions rely solely on human activities to harvest biomechanical and biochemical energy, making them insensitive to external environments<sup>39,128–130</sup>. In addition to the two energy harvesters providing higher charging speed, they also exhibit synergistic additive effects, including ‘fast boosting’ and ‘extended harvesting’ effects for the starting and ending processes of the system<sup>130</sup>. At the starting stage of body movement, the TENG module charges the energy-storage units immediately, but the biofuel cell remains inactive until lactate levels spike. The biofuel cell continues to supply power when body

movement is stopped, compensating for the zero output of the dormant TENG. These complementary effects were verified with an on-body hybrid electronic textile system that integrates supercapacitor modules with capacitances of 75, 150 and 300  $\mu\text{F}$ .

### Power management

Device parameter matching and power management circuits are two strategies for effective self-charging. Sometimes, the design of the self-charging system itself involves certain aspects of power management, such as the matching of voltage, current and capacitance to minimize energy loss. Here, according to the output characteristics, we introduce the power management of two representative self-charging systems based on solar cells or TENGs.

### Photo-charging systems

Solar cells output DC and a relatively low voltage ( $\sim 1\text{ V}$ ), which makes voltage matching with the energy-storage units extremely important for effective energy storage, especially for batteries that usually operate at 2–4 V. For batteries, an ideal charging condition matches their charge voltage with the MPP voltage of the solar cells. Such voltage matching can be achieved by employing a solar module, designing tandem solar cells, engineering photoelectrochemistry at the interface or using an external power management circuit.

The simplest method is to fabricate a solar module and integrate it with a battery with a comparable operational voltage. This method avoids the complexity of chemically engineering the semiconductor–electrolyte interface while maintaining the corresponding performance of each component<sup>15,131</sup>. In a two-electrode photo-charging system, voltage matching can be optimized by developing tandem solar cells with properly matched electrolyte and electrode materials, such as redox couple pairs for a given photo-electrode<sup>132</sup>. Although this optimized voltage matching has only been demonstrated in a solar flow battery using an aqueous organic electrolyte, it provides a better understanding of voltage matching principles and its key role in photo-charging systems<sup>133</sup>.

Power management circuits play a crucial role in the real applications of solar cells. A blocking diode prevents the discharge of current from the energy-storage units into the solar cells, a charge controller avoids overcharging and a converter can regulate the output power or convert the DC output to AC output (FIG. 4a). DC–DC converters are useful for adjusting the voltage output of the solar cells to ensure constant voltage during charging; typical DC–DC converters include boost converters that increase voltage, buck converters that decrease voltage and switched-capacitor doublers or charge pumps that can achieve higher voltages by using capacitors for accumulating energetic charges (FIG. 4b). A classic example of DC–DC converters is the MPP tracker, which has been broadly employed to maintain the MPP of solar cells<sup>134,135</sup>. For supercapacitors that exhibit a slope-charging voltage instead of a voltage plateau in batteries, MPP tracking will be more important than in the case of charging a battery for achieving dynamic

voltage matching<sup>136</sup>. However, all circuits consume a certain amount of energy to start up. Design and selection of power management circuits should be balanced with energy cost-effectiveness, especially in a small-sized flexible photo-charging system; otherwise, parameter matching by device engineering would be more suitable. For instance, the charging circuit of a supercapacitor can be simplified as a traditional resistor–capacitor circuit, in which the internal resistance of the system and the capacitance of the supercapacitor determine the charging speed for a given solar cell. A capacitance matching effect also exists, in which the charging time increases with the increase in capacitance, while the total efficiency exhibits a saturated value at an optimal point<sup>70</sup>.

### Mechano-charging systems

Most TENGs generate pulsed AC outputs with high peak voltages up to the kV level and low current at the  $\mu\text{A}$  level, and require at least a rectifier to convert AC to DC for self-charging. Impedance mismatch between TENGs ( $\text{M}\Omega$ – $\text{G}\Omega$ ) and the energy-storage units (usually below  $100\ \Omega$ ) is an inherent problem that hinders efficient charging<sup>80–82,137,138</sup>. Generally, the power management for a TENG-based self-charging system involves one or some of these processes through device designs and circuits: converting AC to DC, boosting charge, stepping down voltage and stabilizing voltage (FIG. 4c).

The AC output of TENGs can be converted into DC by rectification, including full-wave, half-wave and Bennet's charge doubler voltage rectification (FIG. 4d). Full-wave bridge rectifiers, the most widely applied circuits, contain four individual rectifying diodes connected in a closed loop to conduct rectification. A half-wave rectifier can supplement charges to increase the device voltage and charge and has shown a higher maximum output than full-wave rectification in a capacitive load<sup>139–142</sup>. Alternatively, Bennet's charge doubler can increase the energy output of TENGs to orders of magnitude higher than the full-wave and half-wave rectifications, using diodes as automatic switches for the charge-storage capacitor<sup>143</sup>.

A charge pump can effectively improve the maximum charge density of TENGs, which is usually limited to approximately  $250\ \mu\text{C cm}^{-2}$  by air breakdown. A normal TENG serving as a pump can generate a high voltage and charge an inner-plane-parallel capacitor, which exports electrical energy to the external circuit<sup>144–147</sup>. Based on this method, charges can accumulate on floating metal layers<sup>144</sup>, dielectric tribo-layers<sup>145</sup>, electrodes<sup>146</sup> or an extended area<sup>147</sup>, achieving high charge densities of  $490$ – $1,630\ \mu\text{C cm}^{-2}$ .

To further maximize the energy conversion efficiency, synchronous switches have been developed to achieve impedance matching before or after rectification; these include mechanical switches<sup>148,149</sup>, electrostatic switches<sup>150</sup>, electrical switches<sup>151</sup> and high-voltage microelectromechanical system plasma switches<sup>152</sup>.

A buck converter is necessary to reduce the high voltage of the TENG for efficient and safe charging. Depending on the design of the circuit, strategies include inductive transformers<sup>153,154</sup>, capacitive transformers<sup>148,155</sup> and their coupling with the aforementioned switches<sup>156</sup>.

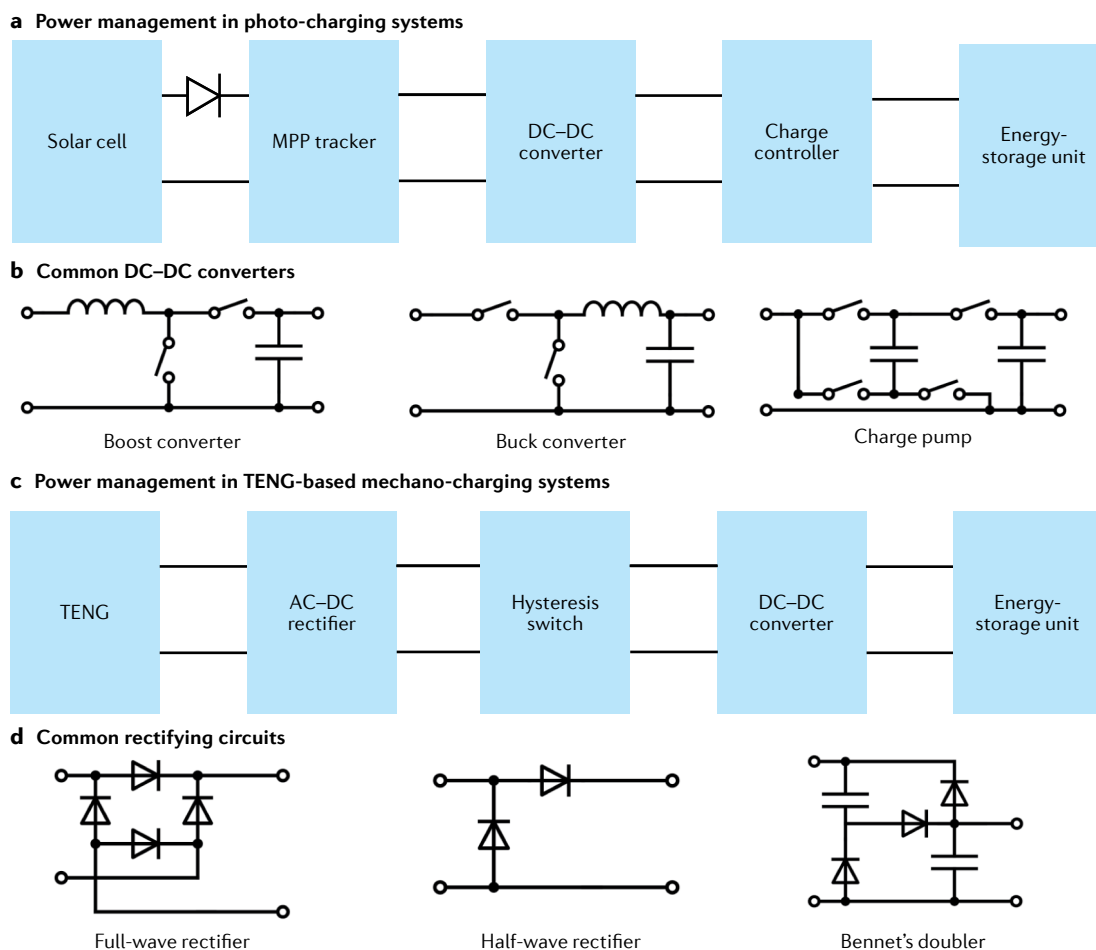


**Fig. 4 | Power management in self-charging power sources.** **a** | Power management circuits in photo-charging systems. A maximum power point (MPP) tracker keeps the solar cells operating at MPP at charging. DC-DC converters can adjust the voltage output of the solar cells to ensure constant voltage during charging. A charge controller is used to prevent overcharging by regulating the voltage and current of solar cells. **b** | Common DC-DC converters. **c** | Power management circuits in triboelectric nanogenerator (TENG)-based mechano-charging systems. AC-DC rectifiers convert the alternating current of TENGs that periodically reverse direction to one direction. Synchronous switches can achieve impedance matching between TENGs and the energy-storage devices before or after rectification. **d** | Typical rectifying circuits for AC-DC conversion. AC, alternating current; DC, direct current.

A two-stage power management circuit was first developed to solve the impedance mismatch problem, in which a temporary capacitor with lower capacitance was charged by the rectified TENG and then transferred energy to the final energy-storage device with high capacitance at an impedance match condition<sup>81</sup>. Another circuit consists of a bridge rectifier, an electrostatic vibration switch and an LC module that reduces the impedance of the pulsed TENG to 0.001  $\Omega$  with the maximization of output energy, achieving an energy-storage efficiency of 57.8%<sup>72</sup>. Finally, a regulator is required to obtain a constant and steady DC charging voltage, which can also be powered by a TENG<sup>141,152</sup>.

As the output of different energy harvesters varies considerably in voltage, current and power density, power management is necessary for efficient charging of supercapacitors or batteries. Generally, for wearable applications, the voltages of solar cells, PENGs, TEGs and biofuel cells must be increased, whereas most TENGs require a voltage step-down.

For hybrid-charging systems, power management is essential because of the different electrical outputs. For example, in a hybrid-charging system consisting of a biofuel cell and a TENG, a boost converter increased the voltage of the biofuel cell and a rectifier transformed the AC signals of the TENG, before they were connected in parallel to conduct charging<sup>130</sup>.

### Applications

The most societally valuable application of flexible self-charging power sources is a self-powered sensing system, whose sensors are powered by harvested energy or even activated by external stimuli<sup>1,5,157-159</sup>. Although numerous 'self-powered' devices have been reported, most are active sensors that utilize electrical signals generated from the energy harvesters<sup>28,160-163</sup>, but still require a certain amount of power provided by an external electrical supply or battery to perform the subsequent data acquisition, processing and transfer. An ideal self-powered sensing system that was proposed

a decade ago, for instance, contained energy harvesters, energy-storage devices, sensors or actuators, data processors and/or controllers, and data transmitters and/or receivers<sup>164</sup>. Because it is complex to manage multiple components that involve energy, considerable electrical engineering challenges are encountered in operating a fully self-sustainable, flexible and wireless sensing system. Nevertheless, progress in flexible self-charging power sources has enabled the application of wireless sensing in areas such as health monitoring and human–machine interactions.

### Health monitoring

A health-monitoring system utilizes biosensors that are compatible with the human body, in the form of wearable or implantable devices, to detect physiological or environmental signals in real time. Functionally, a health-monitoring system should perform accurate signal measurements without interference from human motion, which requires at least a certain degree of device flexibility to fit the curvature of the skin or organ. From the perspective of power supply, it is desirable to employ miniaturized, wireless and flexible power sources that do not need charging or replacement to ensure continuous device operation during normal human activities. Thus, self-powered health-monitoring systems are one of the ultimate forms of personal care systems, overseeing critical medical parameters outside the hospital without interrupting daily life<sup>1,165</sup>.

The power consumption of a target device is important to consider in a self-powered system. For example, a pulse oximeter is a common health-monitoring device that detects heart rate and blood oxygen saturation levels by measuring changes in light absorption in the blood at two different wavelengths, requiring an operation current as high as 20 mA during measurement to support the optoelectronic probe<sup>15</sup>. Flexible photo-charging power sources are, thus, highly desirable given the large current output. Self-powered pulse oximetry measurements with high-quality signals have been realized by integrating optoelectronic probes, data processing electronics and a flexible power source consisting of a layered battery and an amorphous silicon solar cell module<sup>15</sup> (FIG. 5a). However, self-powered pulse oximeters that are capable of continuous monitoring are still far from practical implementation because of the limited performance of current devices. For instance, the capacity of this photo-charging battery when applied to a pulse oximeter was calculated to be approximately 40 mAh in the range 3.6–4.1 V, which would be sufficient to power the oximetry sensor for a few hours; however, it took 9.2 h to charge the battery to this level under practical light illumination conditions of 4.6 mW cm<sup>-2</sup>. To reduce the high power consumption, monolithically integrated organic pulse oximetry sensors based on flexible organic light-emitting diodes and organic photodiodes with a power consumption of only 24 μW have been developed through optimized colour-sensitive light propagation within the human skin<sup>166</sup>.

A TENG-based self-powered system can perform underwater motion tracking when integrated with a packaged multichannel wireless signal transmission

module<sup>167</sup> (FIG. 5b). This system comprises four integrated wearable TENGs, a multichannel wireless signal transmission module and a laptop, and real-time signal display is enabled by gathering and transmitting motion signals from different body parts. Reducing the power consumption of the target application plays an equally important role in improving the efficiency of self-charging power sources in continuous vital body-signal monitoring systems<sup>168</sup>.

Self-charging power sources can also be multifunctional. For example, regulating devices generate energy from light, heat or vibration and, in turn, neutralize the human body's discomfort from the environment. A dual-function thermo-charging device worn on the skin can actively cool the skin by up to 6 °C over long time periods, demonstrating the potential of personalized thermoregulation<sup>43</sup> (FIG. 5c). It is easy to envision that a thin photo-charging device could protect the skin from sunburn, a mechano-charging device could be part of a cushion and a biofuel-charging device could help with adjusting the perspiration rate.

### Human–machine interaction

Human–machine interactions vary from simple touch control of smartphones to intelligent authentication and identification, interactive robotic controls, virtual reality and augmented reality. Sensing technologies capable of capturing human motions and transforming them into electrical signals are the basis of human–machine interactions. Wearable self-powered sensing systems that harvest energy as well as generate signals from human motions, heat or fluids can be an ideal platform for real-time smart interactions<sup>169</sup>. For example, a biofuel-powered soft electronic skin with a high output power density of 3.5 mW cm<sup>-2</sup> was successfully developed to wirelessly control the motion of a robotic arm in real time, in which resistive strain sensors monitored the gesture of the human arm<sup>14</sup> (FIG. 5d). Virtual and augmented reality was realized by skin-integrated wireless haptic interfaces capable of softly laminating the curved surfaces of the body to communicate information through localized mechanical vibrations<sup>170</sup>. Such flexible self-powered human–machine interaction systems are in their infancy, but they point to a future trend for better user experience and broader applications.

### Future perspectives

Although flexible self-charging systems are promising, their efficiency remains lower than that of rigid devices. Managing different types of energy devices on a flexible platform demands advances in different aspects, such as materials engineering, device design and power management, to maintain device performance and even achieve synergy<sup>50,130</sup>. Without proper engineering, a highly efficient energy harvester can result in poor energy storage because of mismatch or load loss.

### Materials development

New materials are key to efficient flexible self-charging systems. For example, the PCE of single-junction organic solar cells, which had been pushed to approximately 12% over the past two decades, has dramatically improved

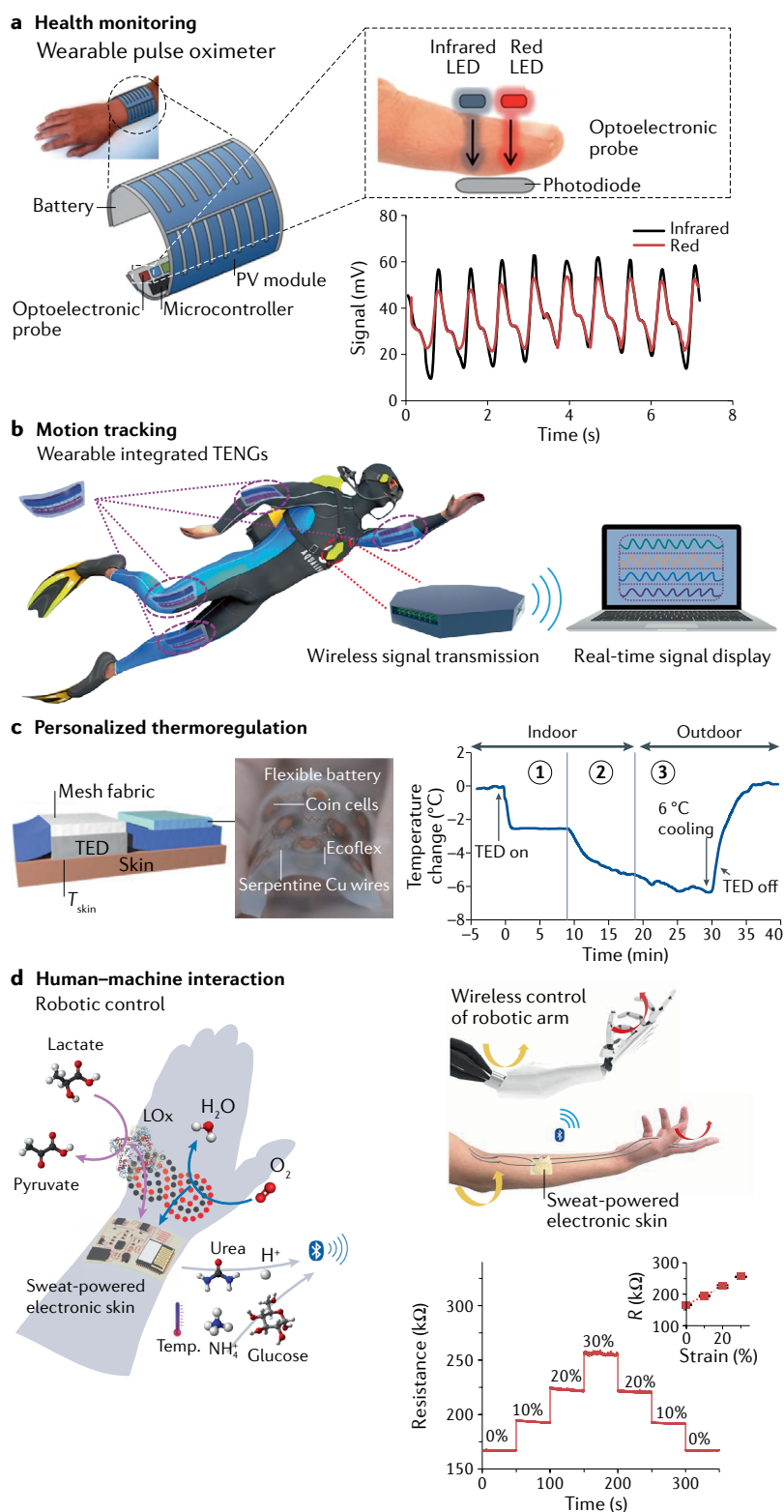


**Fig. 5 | Applications of flexible self-powered sensing systems.** **a** | Health monitoring. A skin pulse oximeter can be driven by photo-charging power sources to detect high-quality signals. The system contains an optoelectronic probe, data processing electronics and a flexible power source consisting of a layered battery and an amorphous silicon solar cell module. The data show that high-quality photoplethysmogram signals can be measured by the self-powered pulse oximeter by using red and infrared light-emitting diodes (LEDs) and a silicon photodiode. **b** | A triboelectric nanogenerator (TENG)-based wearable motion tracking system can perform underwater sensing. It is composed of four integrated wearable TENGs, a multichannel wireless signal transmission module and a laptop. The motion signals of four arthroscases at swimming can be sent to the laptop in real time through assorted software. **c** | An on-skin thermo-charging device can achieve long-term active cooling. The dual-function device integrates a thermoelectric device (TED) cooling armband with a flexible battery pack. The data show that the skin temperature can be changed by TED cooling at sitting (step 1) and walking (steps 2, 3), with a maximum cooling effect of 6 °C. **d** | Human-machine interaction. A biofuel-powered soft electronic skin with a strain sensor can wirelessly control the motion of a robotic arm in real time. The biofuel cell can harvest energy from human sweat to power the strain sensor (laminated on human arm and finger) and send wireless information to control a robotic arm via Bluetooth. The data show resistance response of the strain sensor at different strains. PV, photovoltaic. Panel **a** is adapted from REF.<sup>15</sup>, CC BY 4.0 (<https://creativecommons.org/licenses/by/4.0/>). Panel **b** is adapted from REF.<sup>167</sup>, CC BY 4.0 (<https://creativecommons.org/licenses/by/4.0/>). Panel **c** is reprinted with permission of AAAS from REF.<sup>43</sup>. © The Authors, some rights reserved; exclusive licensee AAAS. Distributed under a CC BY-NC 4.0 License (<http://creativecommons.org/licenses/by-nc/4.0/>). Panel **d** is adapted with permission from REF.<sup>14</sup>, AAAS.

metal oxide films, such as CNTs, conducting polymers, solution-processed metal nanowire networks, printable inks and hybrid components, enable efficient electron transfer between different layers and produce devices with the desired optical and mechanical properties. Progress in these materials is rapidly increasing the efficiency of the devices. Although it has yet to be reported, the realization of self-repairable triboelectrics, supercapacitors and batteries using self-healing polymers is anticipated to produce flexible self-charging systems that can recover their performance from damage or degradation, which would be a significant step towards maintenance-free robust power sources. The materials must also be compatible with mechanical, biomedical and environmental requirements, depending on the application.

### Device design

The design of a flexible integrated device typically includes multiple layers that are required to work normally under a certain degree of repeated mechanical deformation. In such configurations, the relatively thin active layers experience more strain than the rest of the device, which could potentially cause interface mismatches or film cracks. For example, the output performance of energy harvesters such as solar cells and

to 18% in the last 2 years owing to the development of new non-fullerene acceptors. Two-dimensional materials such as layered transition-metal dichalcogenides, carbides, nitrides, oxides and graphene-based materials have enabled very thin active electrodes with high energy density and excellent cyclability for flexible energy-storage devices. Conductive flexible materials other than conventionally deposited metal films or

triboelectrics is less thickness-dependent than that of other devices, because they require only a few hundred nanometres of active materials to absorb light or rely on the electron transfer on the surface. The amount of ions stored in batteries and supercapacitors is greatly affected by the thickness of the active electrode. Hence, devices must be engineered to take into account the differences in device configurations and material tolerances. Using a bridge–island structure or reducing the thicknesses of the substrate and active layers are effective solutions for improving the mechanical flexibility. Emerging device fabrication technologies, such as advanced printing, laser writing and roll-to-roll processing, are important for scalability, miniaturization and monolithic integration.

### General standards

General standards to evaluate the electrical performance of integrated devices at the system level are required at this early stage, owing to the differences in materials, device configurations and energy sources between the components. The concept of total efficiency is simple but not fully comprehensive across an integrated device or accessible to all systems. The PCE under AM 1.5 G conditions is a clear indicator of the output of solar cells but the total efficiency of a photo-charging system varies with the charging time, because the energy-storage efficiency and volumetric capacity must be considered for batteries or supercapacitors. No shared protocols yet exist for calculating the efficiency of triboelectrics, piezoelectrics and biofuel cells, because it is complicated to quantify the energy source under a standard set of conditions, such as AM 1.5 G and  $100 \text{ mW cm}^{-2}$  for solar cells. The alternating output characteristics and diversity of triboelectrics and piezoelectrics also make it difficult to compare their performances within the same framework. Despite the different types of devices, the input energy, charging time, calculated discharge energy and device size are common critical factors that greatly influence the performance. For devices without a constant power output, the average output must be calculated over a stabilized period with quantitative energy input, thereby, avoiding complexity. As the system contains multiple devices, volumetric densities based on the whole weight or size are better than areal densities. These guidelines will help to create an effective assessment to evaluate and compare the general output performance of flexible self-charging systems based on their components.

### Reducing energy loss

Most current self-charging systems suffer from considerable energy loss during the energy transfer process, owing to the lack of proper power management. Although some energy loss is inevitable, power management circuits such as buck converters and boost converters have successfully improved the efficiency of energy transfer in triboelectrics and solar-cell-based self-charging systems through energy accumulation or power maximization, respectively<sup>81,136</sup>. However, designing compatible flexible circuits is challenging, and the power consumption of the circuit is also a concern. Voltage or impedance matching of energy harvesting

and storage devices is an effective and simple method for reducing energy losses during charging. For example, without a circuit, total efficiency can be improved by rationally matching the MPP voltage of a solar module with the charging voltage of an aluminium-ion battery<sup>131</sup>. Other factors such as internal resistance and electrical leakage should be minimized.

### Application requirements

Components must suit specific power requirements and application scenarios. The power consumption of most sensors is at the mW level, which is within the power-generating capability of wearable self-charging power sources. One of the most challenging power tasks for a self-powered sensing system is wireless transmission; the power consumption can vary from a few to hundreds of milliwatts, depending on the module types and transmission distance. Power management circuits also regulate electrical components at the cost of microwatts-level to milliwatts-level power consumption. Hence, whether constant or not, the output of a self-charging power source should at least reach a few tens of milliwatts to support a fully independent wearable device. Because the system converts energy from the ambient environment, harvesters should be designed with access to energy sources. Biofuel cells and thermoelectrics, which convert energy from body fluids and heat, are the best choices for on-skin applications, whereas triboelectrics and piezoelectrics efficiently power *in vivo* bioelectronics by harvesting mechanical energy from the natural contractions and relaxations of the organs or body. Flexible solar cells are an ideal choice if attached to wearable devices that receive sufficient light illumination. Batteries and supercapacitors also exhibit input and output properties that differentiate their uses. Special attention must be paid to miniaturization in wearable sensing systems to ensure sufficient comfort and in untethered soft robotics to avoid redundant power consumption or restrained movement. For wearable electronics and biomedical devices, biocompatibility and safety should be the top priority. Hence, a trade-off between the properties of the components and the requirements of target applications is essential for a practical flexible self-charging power source.

### Lifetime matching

A reliable flexible power source should consider not only the lifetimes of the individual parts but also their influences on the integrated system. Device stability has significantly improved with the development of energy harvesting and storage technologies, and some types of flexible devices can operate for years and millions of cycles, such as triboelectrics and supercapacitors. However, different devices exhibit different life cycle durations, so components should be carefully selected with equivalent lifetimes that fit the target applications. Adverse interactions between the component devices are another concern. Biofuel cells and electrochemical energy-storage devices often contain gel electrolytes for ion migration, which would be harmful to water-sensitive devices such as triboelectrics and solar

cells; adopting solid polymeric ion conductors with good conductivity and stability is a promising solution. Efficient encapsulation materials and technologies will be imperative for achieving durable flexible systems that can resist the adverse effects of the device or working environment. Three or more integrated

devices in a hybrid system can compensate for each other, which is very attractive for multifunctional flexible self-charging systems that operate sustainably under various conditions.

Published online: 12 May 2022

- Someya, T. & Amagai, M. Toward a new generation of smart skins. *Nat. Biotechnol.* **37**, 382–388 (2019).
- Rich, S. I., Wood, R. J. & Majidi, C. Untethered soft robotics. *Nat. Electron.* **1**, 102–112 (2018).
- Zamarayeva, A. M. et al. Flexible and stretchable power sources for wearable electronics. *Sci. Adv.* **3**, e1602051 (2017).
- He, J. et al. Scalable production of high-performing woven lithium-ion fibre batteries. *Nature* **597**, 57–63 (2021).
- Ray, T. R. et al. Bio-integrated wearable systems: a comprehensive review. *Chem. Rev.* **119**, 5461–5533 (2019).
- Curjel, R. F. Self-charging solar battery. US patent 4563727 (1986).
- Kanbara, T., Takada, K., Yamamura, Y. & Kondo, S. Photo-rechargeable solid state battery. *Solid State Ion.* **40–41**, 955–958 (1990).
- Anton, S. R., Erturk, A. & Inman, D. J. Multifunctional self-charging structures using piezoceramics and thin-film batteries. *Smart Mater. Struct.* **19**, 115021 (2010).
- Xue, X., Wang, S., Guo, W., Zhang, Y. & Wang, Z. L. Hybridizing energy conversion and storage in a mechanical-to-electrochemical process for self-charging power cell. *Nano Lett.* **12**, 5048–5054 (2012).
- Chen, J. et al. Micro-cable structured textile for simultaneously harvesting solar and mechanical energy. *Nat. Energy* **1**, 16138 (2016).
- Sun, H., Zhang, Y., Zhang, J., Sun, X. & Peng, H. Energy harvesting and storage in 1D devices. *Nat. Rev. Mater.* **2**, 17023 (2017).
- Pu, X. et al. A self-charging power unit by integration of a textile triboelectric nanogenerator and a flexible lithium-ion battery for wearable electronics. *Adv. Mater.* **27**, 2472–2478 (2015).
- Jeeranpan, I., Sempionatto, J. R., Pavinatto, A., You, J.-M. & Wang, J. Stretchable biofuel cells as wearable textile-based self-powered sensors. *J. Mater. Chem. A* **4**, 18342–18353 (2016).
- Yu, Y. et al. Biofuel-powered soft electronic skin with multiplexed and wireless sensing for human-machine interfaces. *Sci. Robot.* **5**, eaaz7946 (2020).
- Ostfeld, A. E., Gaikwad, A. M., Khan, Y. & Arias, A. C. High-performance flexible energy storage and harvesting system for wearable electronics. *Sci. Rep.* **6**, 26122 (2016).
- Kaltenbrunner, M. et al. Flexible high power-per-weight perovskite solar cells with chromium oxide–metal contacts for improved stability in air. *Nat. Mater.* **14**, 1032–1039 (2015).
- Cheng, Y.-B., Pascoe, A., Huang, F. & Peng, Y. Print flexible solar cells. *Nature* **539**, 488–489 (2016).
- Jinno, H. et al. Stretchable and waterproof elastomer-coated organic photovoltaics for washable electronic textile applications. *Nat. Energy* **2**, 780–785 (2017).
- Kaltenbrunner, M. et al. Ultrathin and lightweight organic solar cells with high flexibility. *Nat. Commun.* **3**, 770 (2012).
- Wu, S. et al. Low-bandgap organic bulk-heterojunction enabled efficient and flexible perovskite solar cells. *Adv. Mater.* **33**, 2105539 (2021).
- Wan, J. et al. Solution-processed transparent conducting electrodes for flexible organic solar cells with 16.61% efficiency. *Nanomicro Lett.* **13**, 44 (2021).
- Kim, S. et al. High-power and flexible indoor solar cells via controlled growth of perovskite using a greener antisolvent. *ACS Appl. Energy Mater.* **3**, 6995–7003 (2020).
- Huang, J. et al. Stretchable ITO-free organic solar cells with intrinsic anti-reflection substrate for high-efficiency outdoor and indoor energy harvesting. *Adv. Funct. Mater.* **31**, 2010172 (2021).
- Zou, H. et al. Quantifying and understanding the triboelectric series of inorganic non-metallic materials. *Nat. Commun.* **11**, 2093 (2020).
- Fan, F.-R., Tian, Z.-Q. & Wang, Z. L. Flexible triboelectric generator. *Nano Energy* **1**, 328–334 (2012).
- Zhu, G. et al. A shape-adaptive thin-film-based approach for 50% high-efficiency energy generation through micro-grating sliding electrification. *Adv. Mater.* **26**, 3788–3796 (2014).
- Deng, J. et al. Vitrimers elastomer-based jigsaw puzzle-like healable triboelectric nanogenerator for self-powered wearable electronics. *Adv. Mater.* **30**, 1705918 (2018).
- Liu, R. et al. Shape memory polymers for body motion energy harvesting and self-powered mechanosensing. *Adv. Mater.* **30**, 1705195 (2018).
- Hinche, R. et al. Transcutaneous ultrasound energy harvesting using capacitive triboelectric technology. *Science* **365**, 491–494 (2019).
- Parida, K. et al. Extremely stretchable and self-healing conductor based on thermoplastic elastomer for all-three-dimensional printed triboelectric nanogenerator. *Nat. Commun.* **10**, 2158 (2019).
- Wang, Z. L. & Song, J. Piezoelectric nanogenerators based on zinc oxide nanowire arrays. *Science* **312**, 242–246 (2006).
- Wu, W. et al. Piezoelectricity of single-atomic-layer MoS<sub>2</sub> for energy conversion and piezotronics. *Nature* **514**, 470–474 (2014).
- Hwang, G.-T. et al. Self-powered deep brain stimulation via a flexible PIMNT energy harvester. *Energy Environ. Sci.* **8**, 2677–2684 (2015).
- Khan, H. et al. Liquid metal-based synthesis of high performance monolayer SnS piezoelectric nanogenerators. *Nat. Commun.* **11**, 3449 (2020).
- Gu, L. et al. Enhancing the current density of a piezoelectric nanogenerator using a three-dimensional intercalation electrode. *Nat. Commun.* **11**, 1030 (2020).
- Park, K.-I. et al. Highly-efficient, flexible piezoelectric PZT thin film nanogenerator on plastic substrates. *Adv. Mater.* **26**, 2514–2520 (2014).
- Hinterleitner, B. et al. Thermoelectric performance of a metastable thin-film Heusler alloy. *Nature* **576**, 85–90 (2019).
- Jin, Q. et al. Flexible layer-structured Bi<sub>2</sub>Te<sub>3</sub> thermoelectric on a carbon nanotube scaffold. *Nat. Mater.* **18**, 62–68 (2019).
- Han, C.-G. et al. Giant thermopower of ionic gelatin near room temperature. *Science* **368**, 1091–1098 (2020).
- He, S. et al. Semiconductor glass with superior flexibility and high room temperature thermoelectric performance. *Sci. Adv.* **6**, eaaz8423 (2020).
- Shi, X.-L., Zou, J. & Chen, Z.-G. Advanced thermoelectric design: from materials and structures to devices. *Chem. Rev.* **120**, 7399–7515 (2020).
- Oh, J. Y. et al. Chemically exfoliated transition metal dichalcogenide nanosheet-based wearable thermoelectric generators. *Energy Environ. Sci.* **9**, 1696–1705 (2016).
- Hong, S. et al. Wearable thermoelectrics for personalized thermoregulation. *Sci. Adv.* **5**, eaaw0536 (2019).
- Lee, B. et al. High-performance compliant thermoelectric generators with magnetically self-assembled soft heat conductors for self-powered wearable electronics. *Nat. Commun.* **11**, 5948 (2020).
- Byun, S.-H. et al. Design strategy for transformative electronic system toward rapid, bidirectional stiffness tuning using graphene and flexible thermoelectric device interfaces. *Adv. Mater.* **33**, 2007239 (2021).
- Bandodkar, A. J. et al. Soft, stretchable, high power density electronic skin-based biofuel cells for scavenging energy from human sweat. *Energy Environ. Sci.* **10**, 1581–1589 (2017).
- Bandodkar, A. J. et al. Battery-free, skin-interfaced microfluidic/electronic systems for simultaneous electrochemical, colorimetric, and volumetric analysis of sweat. *Sci. Adv.* **5**, eaav3294 (2019).
- Tang, S. et al. Enzyme-powered Janus platelet cell robots for active and targeted drug delivery. *Sci. Robot.* **5**, eaba6137 (2020).
- Xu, C., Wang, X. & Wang, Z. L. Nanowire structured hybrid cell for concurrently scavenging solar and mechanical energies. *J. Am. Chem. Soc.* **131**, 5866–5872 (2009).
- Seo, B., Cha, Y., Kim, S. & Choi, W. Rational design for optimizing hybrid thermo-triboelectric generators targeting human activities. *ACS Energy Lett.* **4**, 2069–2074 (2019).
- Qiu, C., Wu, F., Lee, C. & Yuce, M. R. Self-powered control interface based on Gray code with hybrid triboelectric and photovoltaics energy harvesting for IoT smart home and access control applications. *Nano Energy* **70**, 104456 (2020).
- Lukatskaya, M. R. et al. Ultra-high-rate pseudocapacitive energy storage in two-dimensional transition metal carbides. *Nat. Energy* **2**, 17105 (2017).
- Berggren, M. & Malliaras, G. G. How conducting polymer electrodes operate. *Science* **364**, 233–234 (2019).
- Anasori, B., Lukatskaya, M. R. & Gogotsi, Y. 2D metal carbides and nitrides (MXenes) for energy storage. *Nat. Rev. Mater.* **2**, 16098 (2017).
- Armand, M. & Tarascon, J. M. Building better batteries. *Nature* **451**, 652–657 (2008).
- Pomerantseva, E., Bonaccorso, F., Feng, X., Cui, Y. & Gogotsi, Y. Energy storage: the future enabled by nanomaterials. *Science* **366**, eaan8285 (2019).
- Goodenough, J. B. How we made the Li-ion rechargeable battery. *Nat. Electron.* **1**, 204–204 (2018).
- Ma, L. et al. Realizing high zinc reversibility in rechargeable batteries. *Nat. Energy* **5**, 743–749 (2020).
- Simon, P., Gogotsi, Y. & Dunn, B. Where do batteries end and supercapacitors begin? *Science* **343**, 1210–1211 (2014).
- Dubal, D. P., Ayyad, O., Ruiz, V. & Gomez-Romero, P. Hybrid energy storage: the merging of battery and supercapacitor chemistries. *Chem. Soc. Rev.* **44**, 1777–1790 (2015).
- Lukatskaya, M. R., Dunn, B. & Gogotsi, Y. Multidimensional materials and device architectures for future hybrid energy storage. *Nat. Commun.* **7**, 12647 (2016).
- Amatucci, G. G., Badway, F., Du Pasquier, A. & Zheng, T. An asymmetric hybrid nonaqueous energy storage cell. *J. Electrochem. Soc.* **148**, A930 (2001).
- Tie, D. et al. Hybrid energy storage devices: advanced electrode materials and matching principles. *Energy Storage Mater.* **21**, 22–40 (2019).
- Simon, P. & Gogotsi, Y. Perspectives for electrochemical capacitors and related devices. *Nat. Mater.* **19**, 1151–1163 (2020).
- Mackanic, D. G., Kao, M. & Bao, Z. Enabling deformable and stretchable batteries. *Adv. Energy Mater.* **10**, 2001424 (2020).
- Hauch, A., Georg, A., Krašovec, U. O. & Orel, B. Photovoltaically self-charging battery. *J. Electrochem. Soc.* **149**, A1208 (2002).
- Miyasaka, T. & Murakami, T. N. The photocapacitor: an efficient self-charging capacitor for direct storage of solar energy. *Appl. Phys. Lett.* **85**, 3932–3934 (2004).
- Liu, R. et al. Silicon nanowire/polymer hybrid solar cell-supercapacitor: a self-charging power unit with a total efficiency of 10.5%. *Nano Lett.* **17**, 4240–4247 (2017).
- Liang, J. et al. MoS<sub>2</sub>-based all-purpose fibrous electrode and self-powering energy fiber for efficient energy harvesting and storage. *Adv. Energy Mater.* **7**, 1601208 (2017).
- Liu, R. et al. An efficient ultra-flexible photo-charging system integrating organic photovoltaics and supercapacitors. *Adv. Energy Mater.* **10**, 2000523 (2020).
- Li, W., Fu, H.-C., Zhao, Y., He, J.-H. & Jin, S. 14.1% efficient monolithically integrated solar flow battery. *Chem* **4**, 2644–2657 (2018).

72. Qin, H. et al. A universal and passive power management circuit with high efficiency for pulsed triboelectric nanogenerator. *Nano Energy* **68**, 104372 (2020).
73. Segev, G., Beeman, J. W., Greenblatt, J. B. & Sharp, I. D. Hybrid photoelectrochemical and photovoltaic cells for simultaneous production of chemical fuels and electrical power. *Nat. Mater.* **17**, 1115–1121 (2018).
74. Huang, K. et al. High-performance flexible perovskite solar cells via precise control of electron transport layer. *Adv. Energy Mater.* **9**, 1901419 (2019).
75. Ru, P. et al. High electron affinity enables fast hole extraction for efficient flexible inverted perovskite solar cells. *Adv. Energy Mater.* **10**, 1903487 (2020).
76. Giustino, F. & Snaith, H. J. Toward lead-free perovskite solar cells. *ACS Energy Lett.* **1**, 1233–1240 (2016).
77. Ke, W. & Kanatzidis, M. G. Prospects for low-toxicity lead-free perovskite solar cells. *Nat. Commun.* **10**, 965 (2019).
78. Sun, Y. et al. Flexible organic photovoltaics based on water-processed silver nanowire electrodes. *Nat. Electron.* **2**, 513–520 (2019).
79. Qin, F. et al. Robust metal ion-chelated polymer interfacial layer for ultraflexible non-fullerene organic solar cells. *Nat. Commun.* **11**, 4508 (2020).
80. Niu, S. et al. Simulation method for optimizing the performance of an integrated triboelectric nanogenerator energy harvesting system. *Nano Energy* **8**, 150–156 (2014).
81. Niu, S., Wang, X., Yi, F., Zhou, Y. S. & Wang, Z. L. A universal self-charging system driven by random biomechanical energy for sustainable operation of mobile electronics. *Nat. Commun.* **6**, 8975 (2015).
82. Cheng, X. et al. Power management and effective energy storage of pulsed output from triboelectric nanogenerator. *Nano Energy* **61**, 517–532 (2019).
83. Wang, J. et al. A flexible fiber-based supercapacitor–triboelectric-nanogenerator power system for wearable electronics. *Adv. Mater.* **27**, 4830–4836 (2015).
84. Pu, X. et al. Wearable self-charging power textile based on flexible yarn supercapacitors and fabric nanogenerators. *Adv. Mater.* **28**, 98–105 (2016).
85. Liu, M. et al. High-energy asymmetric supercapacitor yarns for self-charging power textiles. *Adv. Funct. Mater.* **29**, 1806298 (2019).
86. Chen, J. et al. Traditional weaving craft for one-piece self-charging power textile for wearable electronics. *Nano Energy* **50**, 536–543 (2018).
87. Dong, K. et al. A highly stretchable and washable all-yarn-based self-charging knitting power textile composed of fiber triboelectric nanogenerators and supercapacitors. *ACS Nano* **11**, 9490–9499 (2017).
88. Cong, Z. et al. Stretchable coplanar self-charging power textile with resist-dyeing triboelectric nanogenerators and microsupercapacitors. *ACS Nano* **14**, 5590–5599 (2020).
89. Wang, S. et al. Motion charged battery as sustainable flexible-power-unit. *ACS Nano* **7**, 11263–11271 (2013).
90. Wang, J. et al. All-plastic-materials based self-charging power system composed of triboelectric nanogenerators and supercapacitors. *Adv. Funct. Mater.* **26**, 1070–1076 (2016).
91. Song, Y. et al. Integrated self-charging power unit with flexible supercapacitor and triboelectric nanogenerator. *J. Mater. Chem. A* **4**, 14298–14306 (2016).
92. Wang, J. et al. Sustainably powering wearable electronics solely by biomechanical energy. *Nat. Commun.* **7**, 12744 (2016).
93. Liu, D. et al. A constant current triboelectric nanogenerator arising from electrostatic breakdown. *Sci. Adv.* **5**, eaav6437 (2019).
94. Chen, C. et al. Direct current fabric triboelectric nanogenerator for biotom energy harvesting. *ACS Nano* **14**, 4585–4594 (2020).
95. Yin, X. et al. A motion vector sensor via direct-current triboelectric nanogenerator. *Adv. Funct. Mater.* **30**, 2002547 (2020).
96. Song, Y. et al. Direct current triboelectric nanogenerators. *Adv. Energy Mater.* **10**, 2002756 (2020).
97. Xue, X. et al. Flexible self-charging power cell for one-step energy conversion and storage. *Adv. Energy Mater.* **4**, 1301329 (2014).
98. Xing, L., Nie, Y., Xue, X. & Zhang, Y. PVDF mesoporous nanostructures as the piezo-separator for a self-charging power cell. *Nano Energy* **10**, 44–52 (2014).
99. Kim, Y.-S. et al. Highly porous piezoelectric PVDF membrane as effective lithium ion transfer channels for enhanced self-charging power cell. *Nano Energy* **14**, 77–86 (2015).
100. Zhou, D., Yang, T., Yang, J. & Fan, L.-Z. A flexible self-charging sodium-ion full battery for self-powered wearable electronics. *J. Mater. Chem. A* **8**, 13267–13276 (2020).
101. Pazhamalai, P. et al. A high efficacy self-charging MoSe<sub>2</sub> solid-state supercapacitor using electrospon nanofibrous piezoelectric separator with ionogel electrolyte. *Adv. Mater. Interfaces* **5**, 1800055 (2018).
102. Zhou, D. et al. A piezoelectric nanogenerator promotes highly stretchable and self-chargeable supercapacitors. *Mater. Horiz.* **7**, 2158–2167 (2020).
103. Krishnamoorthy, K. et al. Probing the energy conversion process in piezoelectric-driven electrochemical self-charging supercapacitor power cell using piezoelectrochemical spectroscopy. *Nat. Commun.* **11**, 2351 (2020).
104. Zhao, D. et al. Ionic thermoelectric supercapacitors. *Energy Environ. Sci.* **9**, 1450–1457 (2016).
105. Kim, S. L., Lin, H. T. & Yu, C. Thermally chargeable solid-state supercapacitor. *Adv. Energy Mater.* **6**, 1600546 (2016).
106. Cheng, H., He, X., Fan, Z. & Ouyang, J. Flexible quasi-solid state ionogels with remarkable Seebeck coefficient and high thermoelectric properties. *Adv. Energy Mater.* **9**, 1901085 (2019).
107. Li, T. et al. Cellulose ionic conductors with high differential thermal voltage for low-grade heat harvesting. *Nat. Mater.* **18**, 608–613 (2019).
108. Dupont, M., MacFarlane, D. & Pringle, J. Thermo-electrochemical cells for waste heat harvesting—progress and perspectives. *Chem. Commun.* **53**, 6288–6302 (2017).
109. Hu, R. et al. Harvesting waste thermal energy using a carbon-nanotube-based thermo-electrochemical cell. *Nano Lett.* **10**, 838–846 (2010).
110. Duan, J. et al. Aqueous thermogalvanic cells with a high Seebeck coefficient for low-grade heat harvest. *Nat. Commun.* **9**, 5146 (2018).
111. Wang, X. et al. Direct thermal charging cell for converting low-grade heat to electricity. *Nat. Commun.* **10**, 4151 (2019).
112. Zhao, C.-E. et al. Nanostructured material-based biofuel cells: recent advances and future prospects. *Chem. Soc. Rev.* **46**, 1545–1564 (2017).
113. Jeerapan, I., Sempionatto, J. R. & Wang, J. On-body bioelectronics: wearable biofuel cells for bioenergy harvesting and self-powered biosensing. *Adv. Funct. Mater.* **30**, 1906243 (2020).
114. Xiao, X. et al. Tackling the challenges of enzymatic (bio)fuel cells. *Chem. Rev.* **119**, 9509–9558 (2019).
115. Agnes, C. et al. Supercapacitor/biofuel cell hybrids based on wired enzymes on carbon nanotube matrices: autonomous reloading after high power pulses in neutral buffered glucose solutions. *Energy Environ. Sci.* **7**, 1884–1888 (2014).
116. Pankratov, D. et al. A Nernstian biosupercapacitor. *Angew. Chem. Int. Ed.* **55**, 15434–15438 (2016).
117. Lv, J. et al. Sweat-based wearable energy harvesting-storage hybrid textile devices. *Energy Environ. Sci.* **11**, 3431–3442 (2018).
118. Qiu, M., Sun, P., Cui, G., Tong, Y. & Mai, W. A flexible microsupercapacitor with integral photocatalytic fuel cell for self-charging. *ACS Nano* **13**, 8246–8255 (2019).
119. Pu, X. et al. Wearable power-textiles by integrating fabric triboelectric nanogenerators and fiber-shaped dye-sensitized solar cells. *Adv. Energy Mater.* **6**, 1601048 (2016).
120. Wen, Z. et al. Self-powered textile for wearable electronics by hybridizing fiber-shaped nanogenerators, solar cells, and supercapacitors. *Sci. Adv.* **2**, e1600097 (2016).
121. Ren, Z. et al. Wearable and self-cleaning hybrid energy harvesting system based on micro/nanostructured haze film. *Nano Energy* **67**, 104243 (2020).
122. Zhang, Q. et al. Shadow enhanced self-charging power system for wave and solar energy harvesting from the ocean. *Nat. Commun.* **12**, 616 (2021).
123. Wu, C. et al. FAPbI<sub>3</sub> flexible solar cells with a record efficiency of 19.38% fabricated in air via ligand and additive synergetic process. *Adv. Funct. Mater.* **29**, 1902974 (2019).
124. Zi, Y. et al. Triboelectric–pyroelectric–piezoelectric hybrid cell for high-efficiency energy-harvesting and self-powered sensing. *Adv. Mater.* **27**, 2340–2347 (2015).
125. Wang, S., Wang, Z. L. & Yang, Y. A one-structure-based hybridized nanogenerator for scavenging mechanical and thermal energies by triboelectric–piezoelectric–pyroelectric effects. *Adv. Mater.* **28**, 2881–2887 (2016).
126. Wu, Y. et al. Triboelectric–thermoelectric hybrid nanogenerator for harvesting energy from ambient environments. *Adv. Mater. Technol.* **3**, 1800166 (2018).
127. Jo, S., Kim, I., Byun, J., Jayababu, N. & Kim, D. Boosting a power performance of a hybrid nanogenerator via frictional heat combining a triboelectricity and thermoelectricity toward advanced smart sensors. *Adv. Mater. Technol.* **6**, 2000752 (2021).
128. Pan, C., Li, Z., Guo, W., Zhu, J. & Wang, Z. L. Fiber-based hybrid nanogenerators for/as self-powered systems in biological liquid. *Angew. Chem. Int. Ed.* **50**, 11192–11196 (2011).
129. Hansen, B. J., Liu, Y., Yang, R. & Wang, Z. L. Hybrid nanogenerator for concurrently harvesting biomechanical and biochemical energy. *ACS Nano* **4**, 3647–3652 (2010).
130. Yin, L. et al. A self-sustainable wearable multi-modular E-textile bioenergy microgrid system. *Nat. Commun.* **12**, 1542 (2021).
131. Hu, Y. et al. A portable and efficient solar-rechargeable battery with ultrafast photo-charge/discharge rate. *Adv. Energy Mater.* **9**, 1900872 (2019).
132. Fu, H.-C. et al. An efficient and stable solar flow battery enabled by a single-junction GaAs photoelectrode. *Nat. Commun.* **12**, 156 (2021).
133. Li, W. & Jin, S. Design principles and developments of integrated solar flow batteries. *Acc. Chem. Res.* **53**, 2611–2621 (2020).
134. Santos, J. L., Antunes, F., Chehab, A. & Cruz, C. A maximum power point tracker for PV systems using a high performance boost converter. *Sol. Energy* **80**, 772–778 (2006).
135. Miyatake, M., Veerachary, M., Toriumi, F., Fujii, N. & Ko, H. Maximum power point tracking of multiple photovoltaic arrays: a PSO approach. *IEEE Trans. Aerosp. Electron. Syst.* **47**, 367–380 (2011).
136. Gurusu, A. et al. Highly efficient perovskite solar cell photocharging of lithium ion battery using DC–DC booster. *Adv. Energy Mater.* **7**, 1602105 (2017).
137. Fang, C. et al. Overview of power management for triboelectric nanogenerators. *Adv. Intell. Syst.* **2**, 1900129 (2020).
138. Niu, S. & Wang, Z. L. Theoretical systems of triboelectric nanogenerators. *Nano Energy* **14**, 161–192 (2015).
139. Xu, L. et al. Giant voltage enhancement via triboelectric charge supplement channel for self-powered electroadhesion. *ACS Nano* **12**, 10262–10271 (2018).
140. Ghaffarnejad, A., Hasani, J. Y., Galayko, D. & Basset, P. Superior performance of half-wave to full-wave rectifier as a power conditioning circuit for triboelectric nanogenerators: application to contact-separation and sliding mode TENG. *Nano Energy* **66**, 104137 (2019).
141. Xu, S. et al. Self-doubled-rectification of triboelectric nanogenerator. *Nano Energy* **66**, 104165 (2019).
142. Li, G. et al. Miura folding based charge-excitation triboelectric nanogenerator for portable power supply. *Nano Res.* **14**, 4204–4210 (2021).
143. Ghaffarnejad, A. et al. A conditioning circuit with exponential enhancement of output energy for triboelectric nanogenerator. *Nano Energy* **51**, 173–184 (2018).
144. Xu, L., Bu, T. Z., Yang, X. D., Zhang, C. & Wang, Z. L. Ultrahigh charge density realized by charge pumping at ambient conditions for triboelectric nanogenerators. *Nano Energy* **49**, 625–633 (2018).
145. Cheng, L., Xu, Q., Zheng, Y., Jia, X. & Qin, Y. A self-improving triboelectric nanogenerator with improved charge density and increased charge accumulation speed. *Nat. Commun.* **9**, 3773 (2018).
146. Liu, W. et al. Integrated charge excitation triboelectric nanogenerator. *Nat. Commun.* **10**, 1426 (2019).
147. He, W. et al. Boosting output performance of sliding mode triboelectric nanogenerator by charge space-accumulation effect. *Nat. Commun.* **11**, 4277 (2020).
148. Zi, Y. et al. An inductor-free auto-power-management design built-in triboelectric nanogenerators. *Nano Energy* **31**, 302–310 (2017).
149. Cheng, G. et al. Managing and maximizing the output power of a triboelectric nanogenerator by controlled tip–electrode air-discharging and application for UV sensing. *Nano Energy* **44**, 208–216 (2018).
150. Yang, J. et al. Managing and optimizing the output performances of a triboelectric nanogenerator

- by a self-powered electrostatic vibrator switch. *Nano Energy* **46**, 220–228 (2018).
151. Cheng, X. et al. High efficiency power management and charge boosting strategy for a triboelectric nanogenerator. *Nano Energy* **38**, 438–446 (2017).
  152. Zhang, H. et al. Employing a MEMS plasma switch for conditioning high-voltage kinetic energy harvesters. *Nat. Commun.* **11**, 3221 (2020).
  153. Zhu, G., Chen, J., Zhang, T., Jing, Q. & Wang, Z. L. Radial-arrayed rotary electrification for high performance triboelectric generator. *Nat. Commun.* **5**, 3426 (2014).
  154. Pu, X. et al. Efficient charging of Li-ion batteries with pulsed output current of triboelectric nanogenerators. *Adv. Sci.* **3**, 1500255 (2016).
  155. Liu, W. et al. Switched-capacitor-convertors based on fractal design for output power management of triboelectric nanogenerator. *Nat. Commun.* **11**, 1883 (2020).
  156. Xi, F. et al. Universal power management strategy for triboelectric nanogenerator. *Nano Energy* **37**, 168–176 (2017).
  157. Park, S. et al. Self-powered ultra-flexible electronics via nano-grating-patterned organic photovoltaics. *Nature* **561**, 516–521 (2018).
  158. Song, Y., Mukasa, D., Zhang, H. & Gao, W. Self-powered wearable biosensors. *Acc. Mater. Res.* **2**, 184–197 (2021).
  159. Zheng, Q., Tang, Q., Wang, Z. L. & Li, Z. Self-powered cardiovascular electronic devices and systems. *Nat. Rev. Cardiol.* **18**, 7–21 (2020).
  160. Lou, Z., Li, L., Wang, L. & Shen, G. Recent progress of self-powered sensing systems for wearable electronics. *Small* **13**, 1701791 (2017).
  161. Chun, K. Y., Son, Y. J., Jeon, E. S., Lee, S. & Han, C. S. A self-powered sensor mimicking slow- and fast-adapting cutaneous mechanoreceptors. *Adv. Mater.* **30**, 1706299 (2018).
  162. Meng, K. et al. A wireless textile-based sensor system for self-powered personalized health care. *Matter* **2**, 896–907 (2020).
  163. Wang, Z. et al. A self-powered angle sensor at nanoradian-resolution for robotic arms and personalized medicine. *Adv. Mater.* **32**, 2001466 (2020).
  164. Wang, Z. L. Self-powered nanosensors and nanosystems. *Adv. Mater.* **24**, 280–285 (2012).
  165. Korhonen, I., Parkka, J. & Van Gils, M. Health monitoring in the home of the future. *IEEE Eng. Med. Biol. Mag.* **22**, 66–73 (2003).
  166. Lee, H. et al. Toward all-day wearable health monitoring: an ultralow-power, reflective organic pulse oximetry sensing patch. *Sci. Adv.* **4**, eaas9530 (2018).
  167. Zou, Y. et al. A bionic stretchable nanogenerator for underwater sensing and energy harvesting. *Nat. Commun.* **10**, 2695 (2019).
  168. Yu, H., Li, N. & Zhao, N. How far are we from achieving self-powered flexible health monitoring systems: an energy perspective. *Adv. Energy Mater.* **11**, 2002646 (2021).
  169. Yin, R., Wang, D., Zhao, S., Lou, Z. & Shen, G. Wearable sensors-enabled human-machine interaction systems: from design to application. *Adv. Funct. Mater.* **31**, 2008936 (2021).
  170. Yu, X. et al. Skin-integrated wireless haptic interfaces for virtual and augmented reality. *Nature* **575**, 473–479 (2019).
  171. Starner, T. Human-powered wearable computing. *IBM Syst. J.* **35**, 618–629 (1996).
  172. Riemer, R. & Shapiro, A. Biomechanical energy harvesting from human motion: theory, state of the art, design guidelines, and future directions. *J. Neuroeng. Rehabil.* **8**, 22 (2011).
  173. Zhou, M., Al-Furjan, M. S. H., Zou, J. & Liu, W. A review on heat and mechanical energy harvesting from human: principles, prototypes and perspectives. *Renew. Sust. Energ. Rev.* **82**, 3582–3609 (2018).
  174. Lee, E. J. et al. High-performance piezoelectric nanogenerators based on chemically-reinforced composites. *Energy Environ. Sci.* **11**, 1425–1430 (2018).
  175. Li, H. et al. A hybrid biofuel and triboelectric nanogenerator for bioenergy harvesting. *Nanomicro Lett.* **12**, 50 (2020).

#### Acknowledgements

This work was supported by JSPS KAKENHI under grant nos. JP18H05465 and JP18H05469.

#### Author contributions

R.L. wrote and edited the article. Z.L.W., K.F. and T.S. contributed to the discussion of content and edited the manuscript before submission.

#### Competing interests

The authors declare no competing interests.

#### Peer review information

*Nature Reviews Materials* thanks Weishu Liu and the other, anonymous, reviewer(s) for their contribution to the peer review of this work.

#### Publisher's note

Springer Nature remains neutral with regard to jurisdictional claims in published maps and institutional affiliations.

© Springer Nature Limited 2022